The GP2014 Ground Motion Simulation Technique

Robert W. Graves
USGS Pasadena

Arben Pitarka
Lawrence Livermore National Laboratory

- Background
- Rupture Characterization
- Low Frequency Simulation
- High Frequency Simulation
- Combine into Broadband
- Research Needs

USGS science for a changing world

What is strong ground motion?

We typically thing of it as 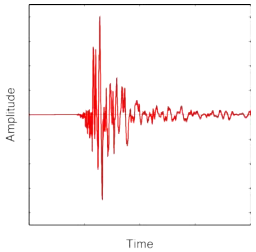

or maybe 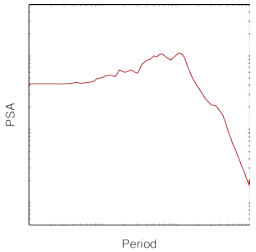

However, for most of the world it is:

Hybrid Approach to Broadband Ground Motion Simulations

Graves and Pitarka (2010)

- Semi-deterministic approach at low frequencies
- Semi-stochastic approach at high frequencies
- Kinematic Rupture Generator
  - Unified scaling rules for rise time, rupture speed and corner frequency
  - Depth scaling of rise time (increase) and rupture speed (decrease) required to model shallow (< 5 km) moment release
- Applied to 1979 Imperial Valley, 1989 Loma Prieta, 1992 Landers and 1994 Northridge events

Refinements to the Graves-Pitarka Broadband Simulation Method

Graves and Pitarka (2014)

- Addition of deep "weak-zone" to rupture characterization
- Perturbation of correlation structure for rise-time and rupture speed
- Extension of methodology to Eastern North America (ENA)

Representation Theorem

$$u_j(t) = \sum G_{ij}(t) * D_i(t)$$

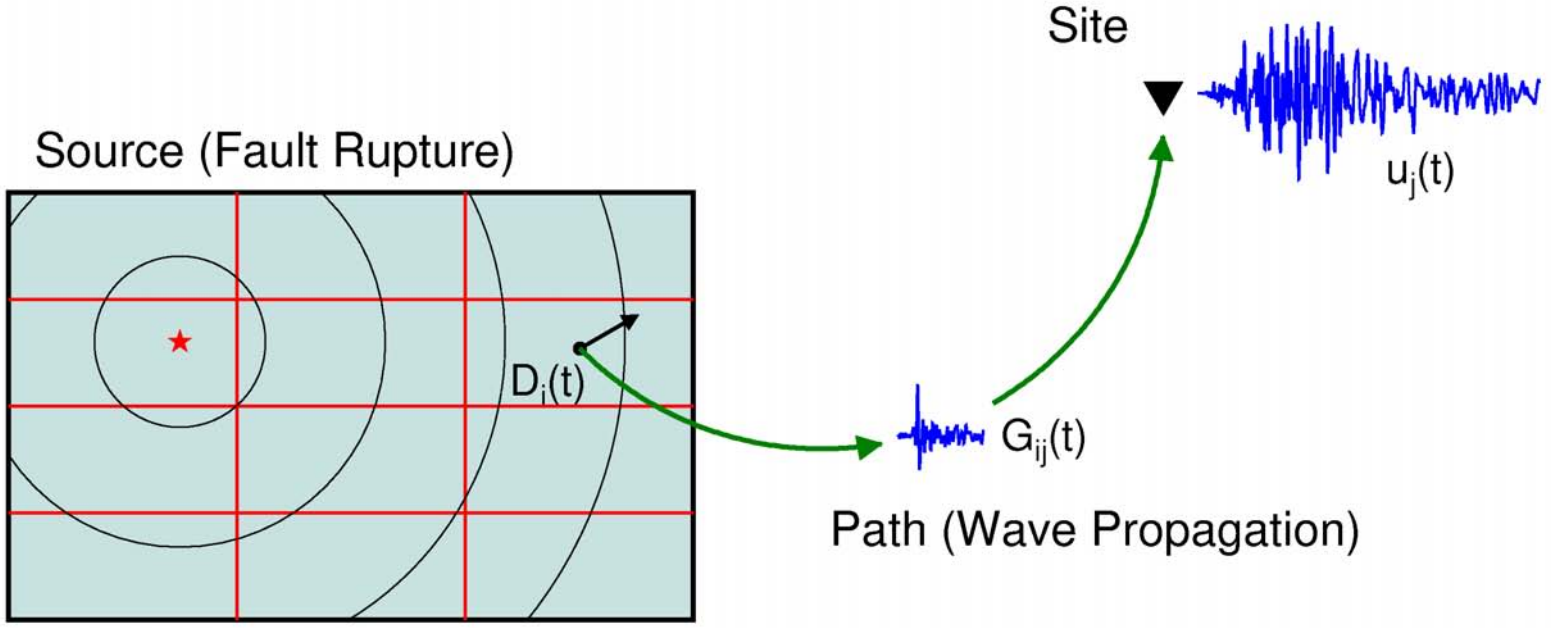

Hybrid Simulation Method

Low Frequency (f < 1 Hz)

Complete kinematic finite-fault rupture description including spatial and temporal heterogeneity in the slip function. Full theoretical Green's functions computed for specified plane-layered or 3D velocity structure including anealstic attenuation.

High Frequency (f > 1 Hz)

Limited kinematic finite-fault rupture description including spatial heterogeneity in slip and rupture time. Each subfault radiates an w^{-2} spectrum with ***stochastic*** phase and conically averaged radiation pattern. Simplified ray path Green's functions include travel time and impedance effects. Frequency dependent attenuation represents both anelastic and scattering effects.

Hybrid approaches have traditionally been labeled using the following nomenclature:

- Low Frequency = **Determinstic**
- High frequency = **Stochastic**

Strictly speaking, the above classification is not correct because both approaches utilize deterministic and stochastic features. For example, the slip distribution used in the low-frequency simulation is generated using a stochastic model. Likewise, travel time and impedance effects in the high-frequency simulation are purely deterministic.

A more accurate representation is:

- Low Frequency = **Comprehensive Theoretical Basis**
- High frequency = **Simplified Theoretical Basis**

Kinematic Rupture Generator

Required inputs (SRC file)

- Magnitude
- Fault length (km)
- Subfault dimension along strike
- Fault width (km)
- Subfault dimension down-dip
- Latitude of top center point
- Longitude of top center point
- Depth to top of fault
- Hypocenter location along strike from top center (km)
- Hypocenter down-dip from top center (km)
- Strike
- Dip
- Rake (average)
- Seed for random number generator
- Time step for slip-rate function

Recommend using Leonard (2010) Magnitude-Area and Magnitude-Length scaling relations for GP method.

Kinematic Rupture Generator

Sample SRC file:

```
MAGNITUDE = 6.94
FAULT_LENGTH = 40.0
DLEN = 0.1
FAULT_WIDTH = 22.0
DWID = 0.1
LAT_TOP_CENTER = 37.0789
LON_TOP_CENTER = -121.8410
DEPTH_TO_TOP = 0.0
HYPO_ALONG_STK = 0.0
HYPO_DOWN_DIP = 14.75
STRIKE = 128
DIP = 70
RAKE = 136
SEED = 1343642
DT = 0.1
```

1. Slip Distribution

- Begin with uniform slip having mild taper at edges.

- Transform to wavenumber domain and use Mai and Beroza (2002) spatial correlation functions with random phasing to filter wavenumber spectrum.

$$A(k_s,k_d) = [a_s\, a_d / (1 + K^2)^{H+1}]^{1/2} \qquad (H = 0.75)$$

$$K^2 = a_s^2 k_s^2 + a_d^2\, k_d^2$$

$$\log_{10} a_s = M_w / 2.0 - 2.5$$

$$\log_{10} a_d = M_w / 3.0 - 1.5$$

- Transform back to spatial domain and scale standard deviation of slip to be 85% of average:

$$s_s = 0.85 \cdot D_{avg}$$

with D_{avg} scaled to give desired M_w

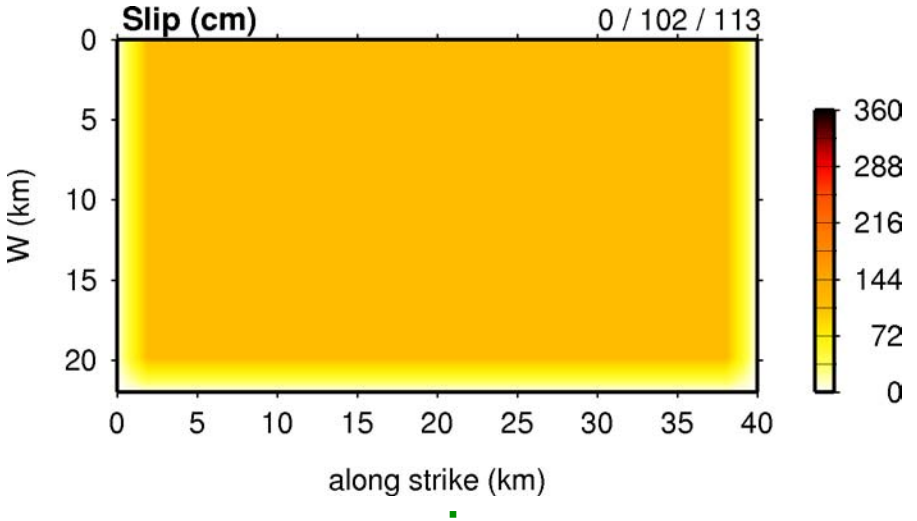

For $M_w = 6.94$
$a_s = 9.3$ km
$a_d = 6.5$ km

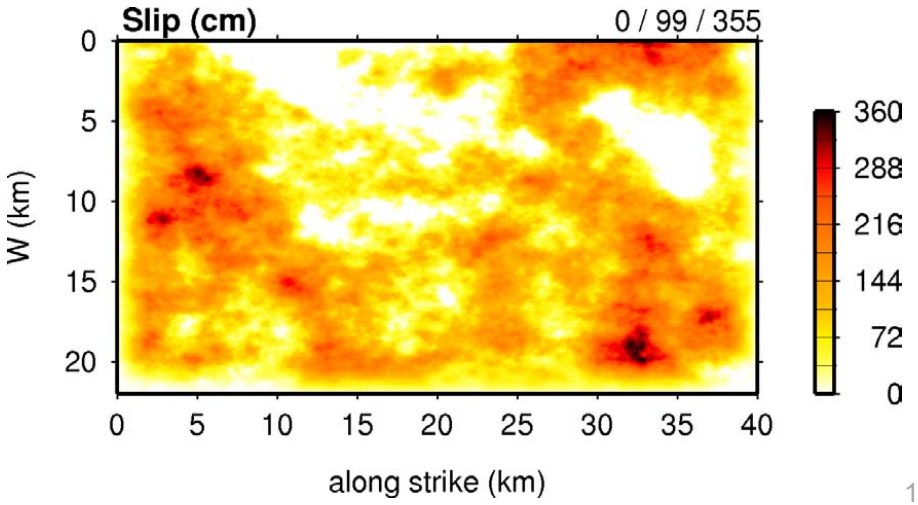

2. Rupture Initiation Time

First, compute background value T_B

$T_B = r_{path} / V_r$

WUS: V_r = 80% local V_s depth > 8 km
= 56% local V_s depth < 5 km
(linear transition between 5-8 km)

ENA: V_r = 85% local V_s all depths

Reduction of V_r above 5 km depth for WUS represents velocity strengthening behavior in weaker near-surface material

Next, add timing adjustment that correlates with local slip

$T_i = T_B - Dt_0(D_i)$

Dt_0 scales with slip amount of i^{th} subfault (D_i) to accelerate or decelerate rupture

$Dt_0(D_{avg}) = 0$

$Dt_0(D_{max}) = 1.8 \times 10^{-9} \cdot M_o^{1/3}$

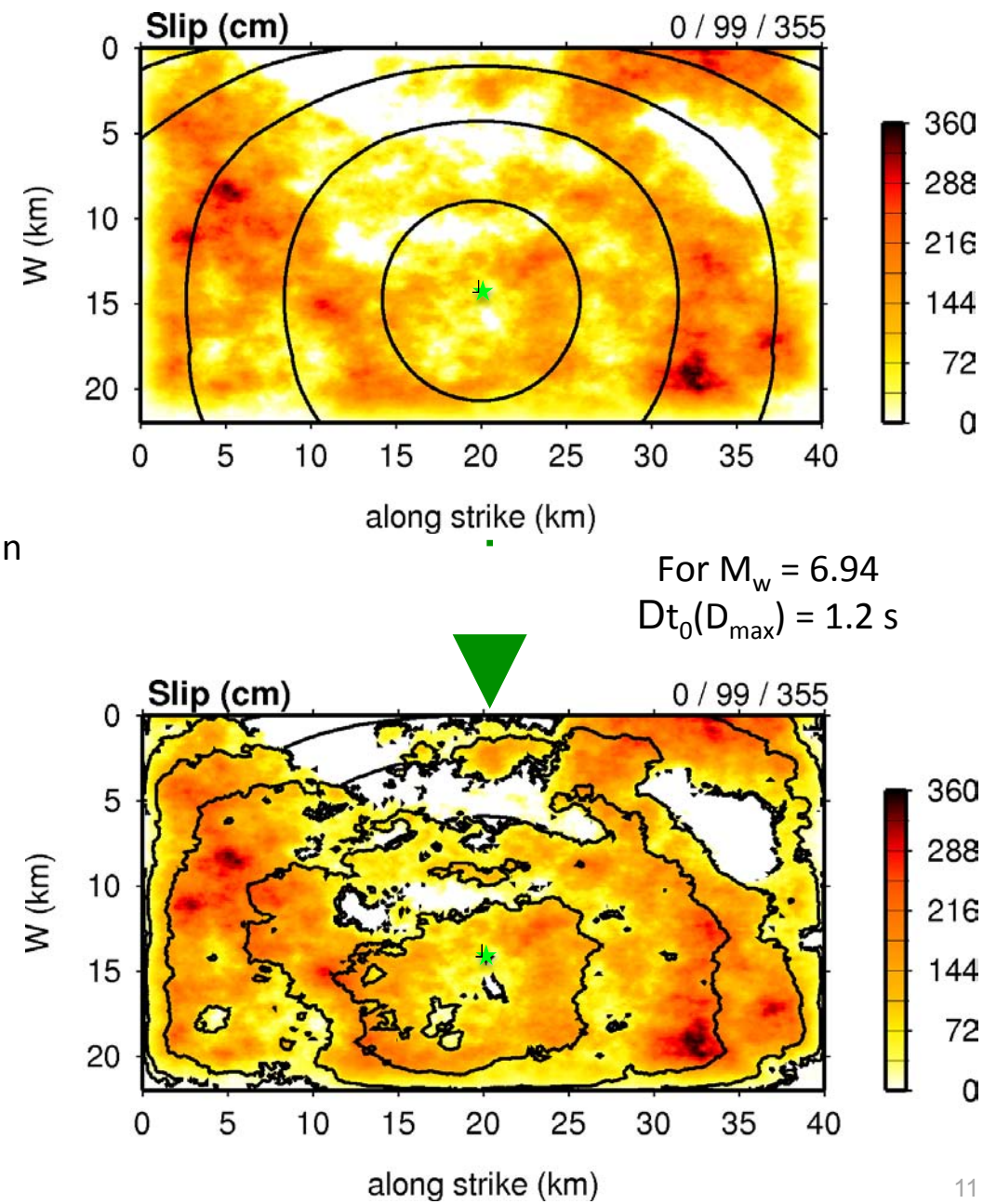

For M_w = 6.94
$Dt_0(D_{max})$ = 1.2 s

2. Rupture Initiation Time

GP2014 adds random perturbations to timing adjustment so it is no longer correlated 1:1 with local slip

$T_i = T_B - Dt_0(D_i) \exp(es_T)$

e: random number selected from standard normal distribution (mean of zero, standard deviation of one)

s_T: log-normal standard deviation

s_T = 0.2 in GP14.3

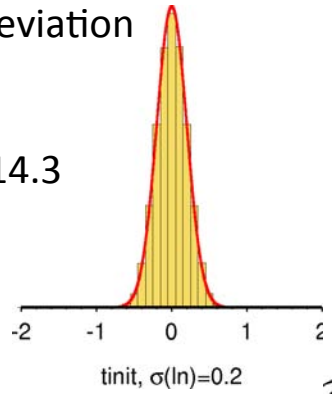

This mimics the short length scale starting and stopping of the rupture as it propagates across the fault, possibly due to geometric complexities and/or stress heterogeneities

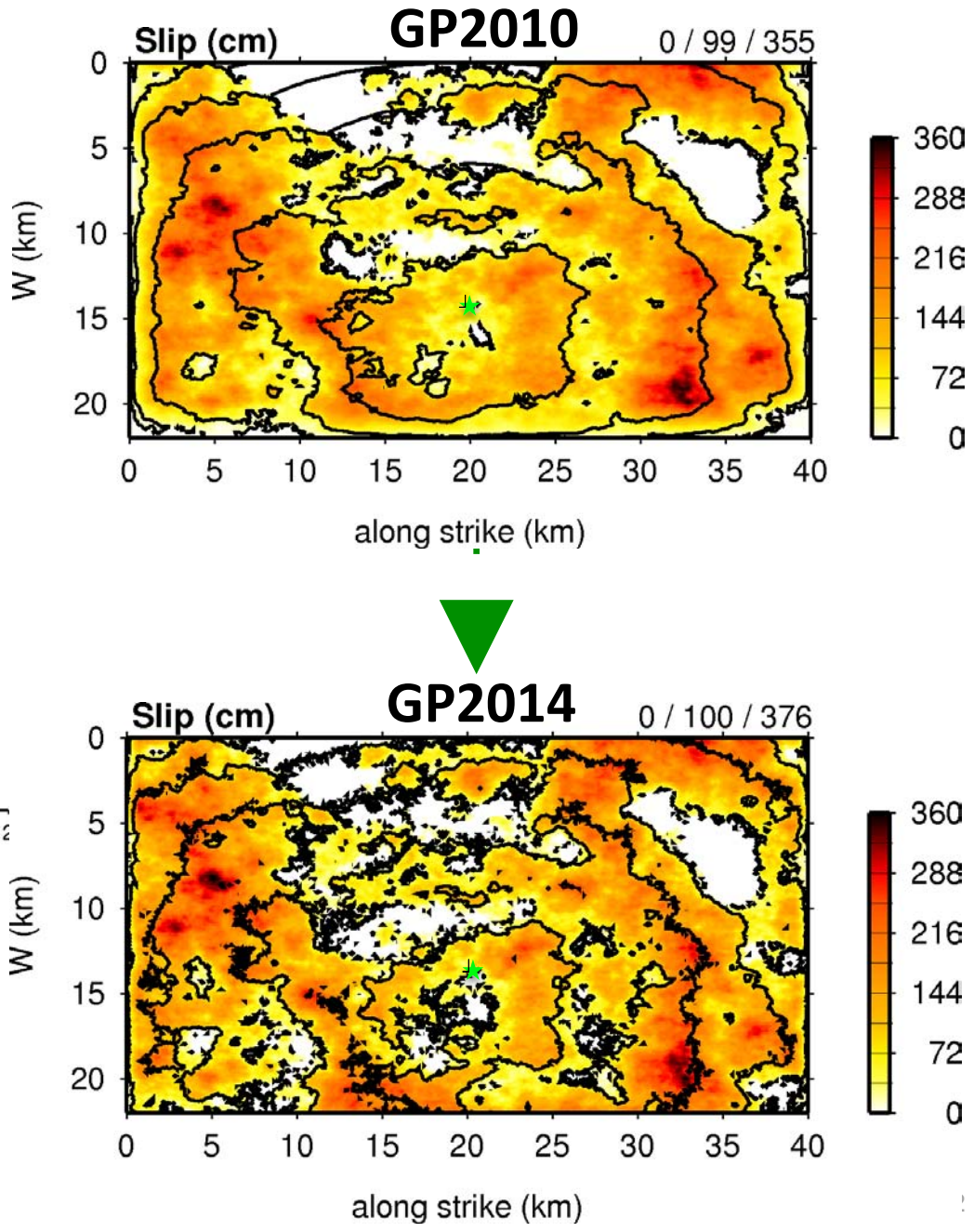

3. Slip Rate Function

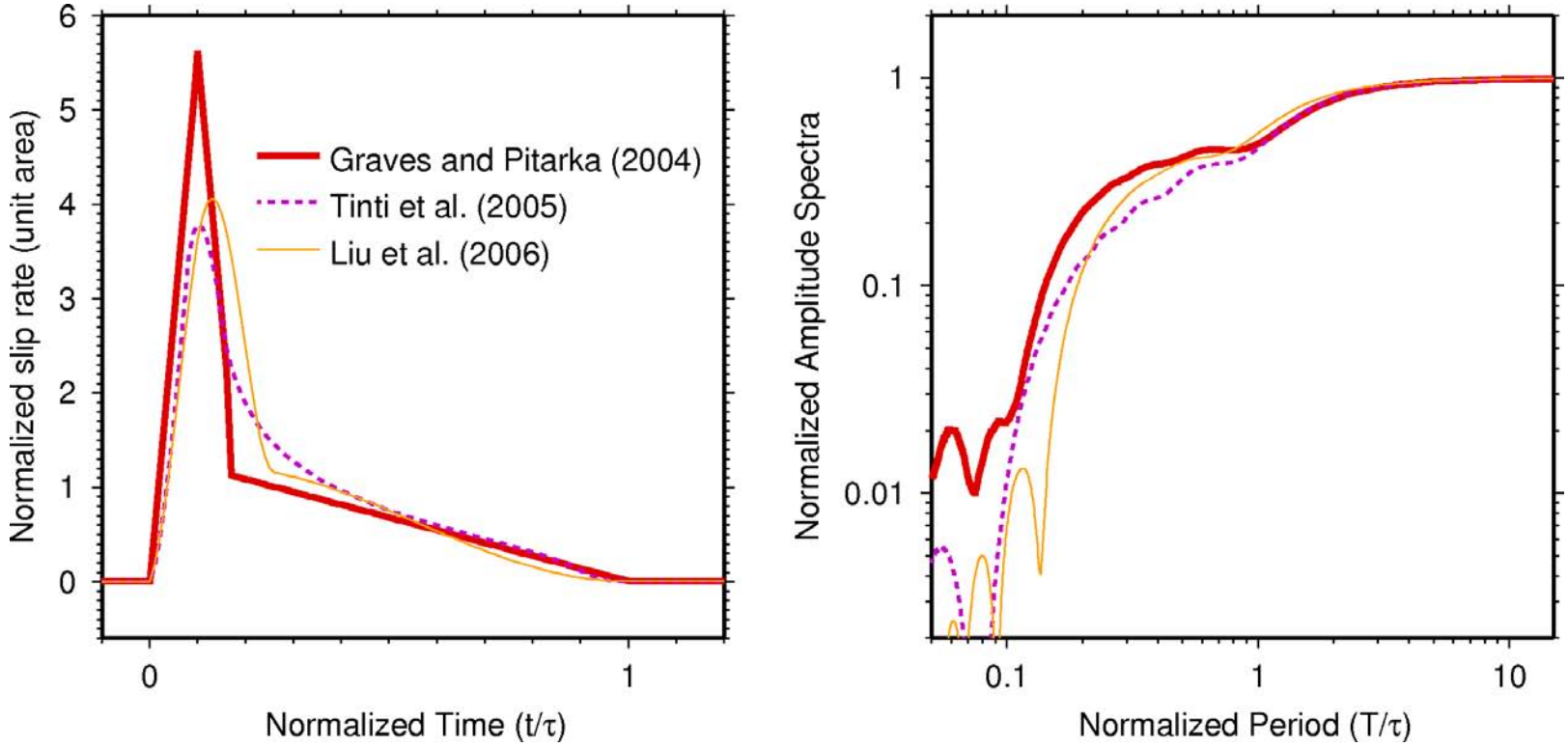

- We have considered several slip-rate functions in the GP methodology. All are "Kostrov-like" meaning they have a sharp rise to the maximum value followed by a lower amplitude, longer period tail.
- In our methodology, the rise time (t) is the total length of the slip-rate function
- At periods around t or longer there is little difference in these functions
- Currently, we use the slip-rate function based on Liu et al (2006)

3. Slip Rate Function

Subfault rise time (t_i) scales with square root of local slip (D_i)

WUS: $t_i = k \cdot D_i^{1/2}$ depth > 8 km
$= 2 \cdot k \cdot D_i^{1/2}$ depth < 5 km
(linear transition between 5-8 km)

ENA: $t_i = k \cdot D_i^{1/2}$ all depths

Lengthening of t_i above 5 km depth in WUS represents velocity strengthening behavior in weaker near-surface material

The constant (k) set so average rise time across entire fault is given by the relation:

$$t_A = a_T \cdot c_1 \times 10^{-9} \cdot M_o^{1/3}$$

where c_1=1.45 in WUS and 2.20 in ENA, and a_T is a mechanism dependent scaling factor (next slide).

The scaling with square root of slip represents a balance between constant rise time at one extreme and constant slip-rate at the other.

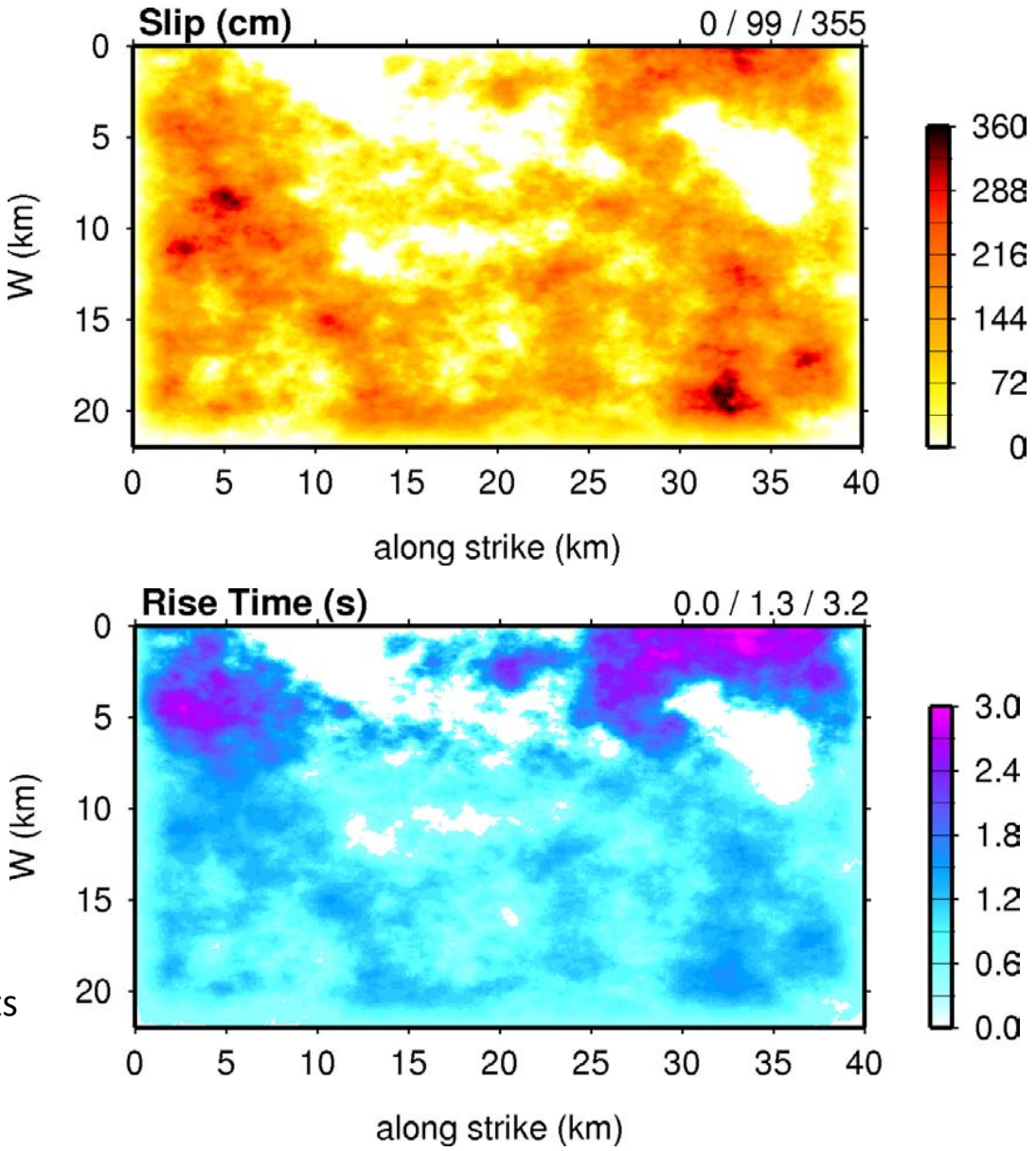

3. Slip Rate Function

GP2014 modifications to rise time:

- The factor a_T scales the rise time as a function of fault dip and rake. The idea is that rupture in compressive regimes (e.g., blind thrust) produces shorter rise times.

$$a_T = [1 + F_D F_R c_a]^{-1}$$

$F_D = 1 - (d - 45^o)/45^o$, $45^o < d \le 90^o$
$= 1$, $d \le 45^o$
$F_R = 1 - |l - 90^o|/90^o$, $0^o \le l \le 180^o$
$= 0$, otherwise
$c_a = 0.1$

min $a_T = 0.91$ for $d \le 45^o$ and $l = 90^o$ (shallow thrust)
max $a_T = 1.0$ for $d = 90^o$ (vertical fault), $l \le 0^o$ (strike-slip/normal)

- For WUS, impose weak zone along the deeper portion of fault with factor of 2 increase in rise time from 15-18 km. Represents transition from unstable to stable sliding in midcrust (e.g., Scholz, 1998)

- Add perturbations to rise time so it is no longer correlated 1:1 with square root of local slip. Mimics short length scale variations possibly due to geometric complexities and/or stress heterogeneities

$$t_{Ri} = t_i \exp(\varepsilon s_t)$$

ε is a random number selected from standard normal distribution
s_t is the log-normal standard deviation

$s_t = 0.5$ in GP14.3

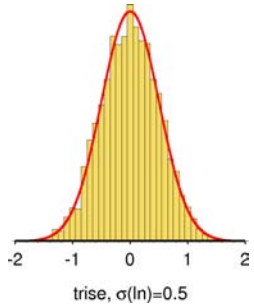

3. Slip Rate Function

GP2014 modifications to rise time:

Goal is to provide a smoother transition between the low- and high-frequency simulation approaches through the addition of stochastic perturbations.

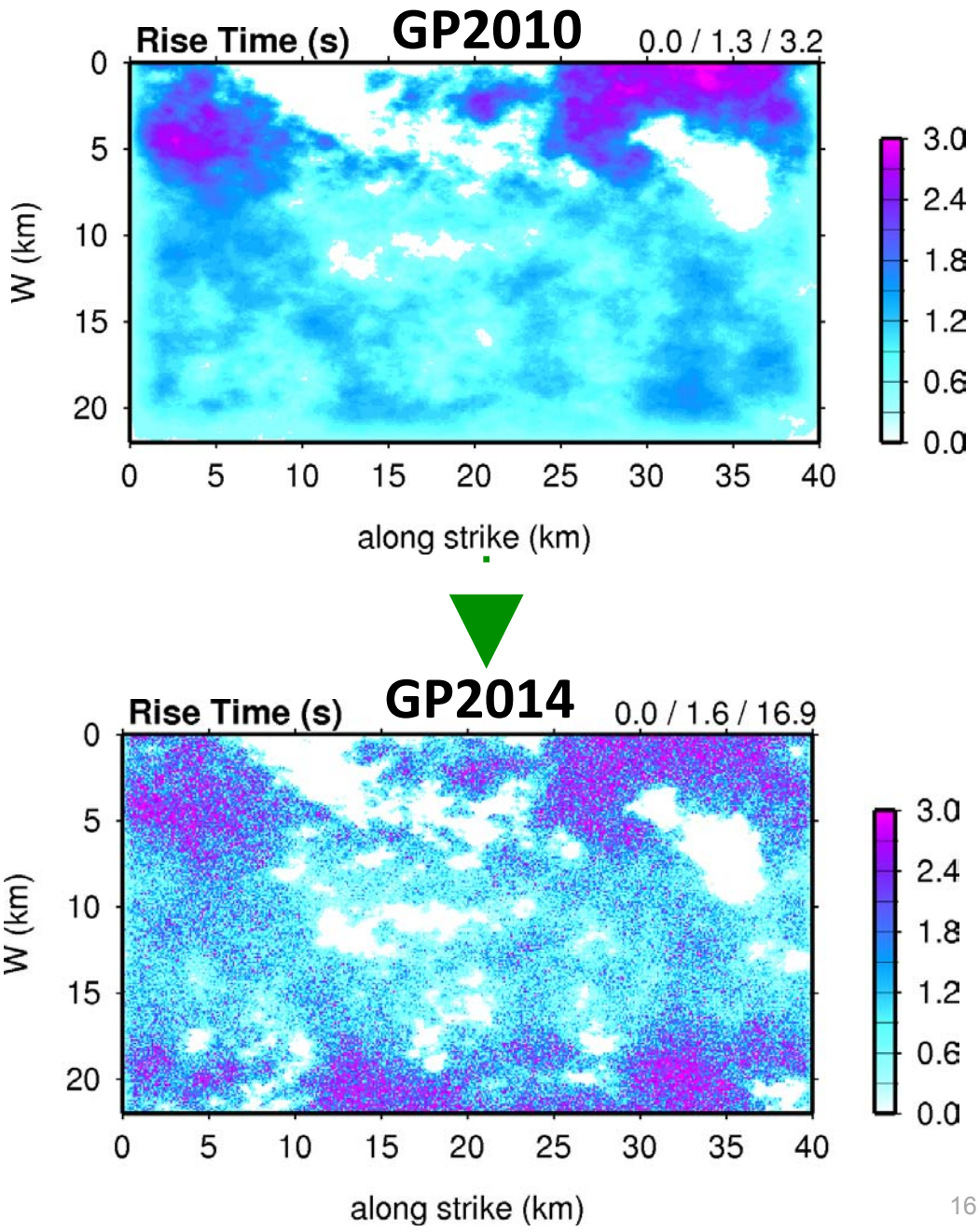

4. Slip Direction (Rake)

Subfault rake (l_i) is given by average value (l_0) plus random perturbations:

$$l_i = l_o + e$$

range: $-60^o < e < 60^o$

standard deviation: $s_e = 15^o$

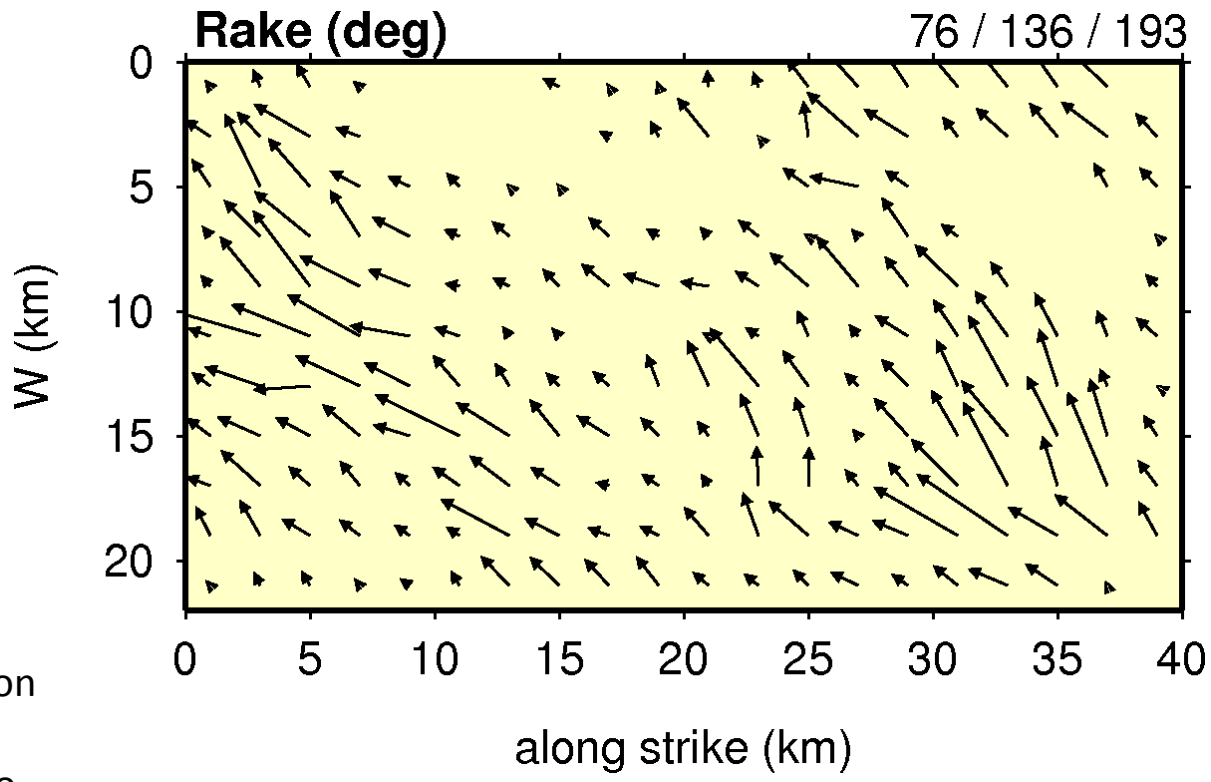

Random perturbations of rake follow spatial distribution given by Mai and Beroza (2002) wavenumber correlation structure (roughly K^{-2} falloff). Uses a different seed than slip distribution so rake variations are not correlated with slip variations.

Example: 1992 Landers EQ

- **Specified parameters**
  - Magnitude, mechanism and hypocenter
  - Fault strike, dip and dimensions
- **Rule Based Parameters**
  - Slip distribution, rise time/corner frequency and rake
  - Scale with depth and local slip

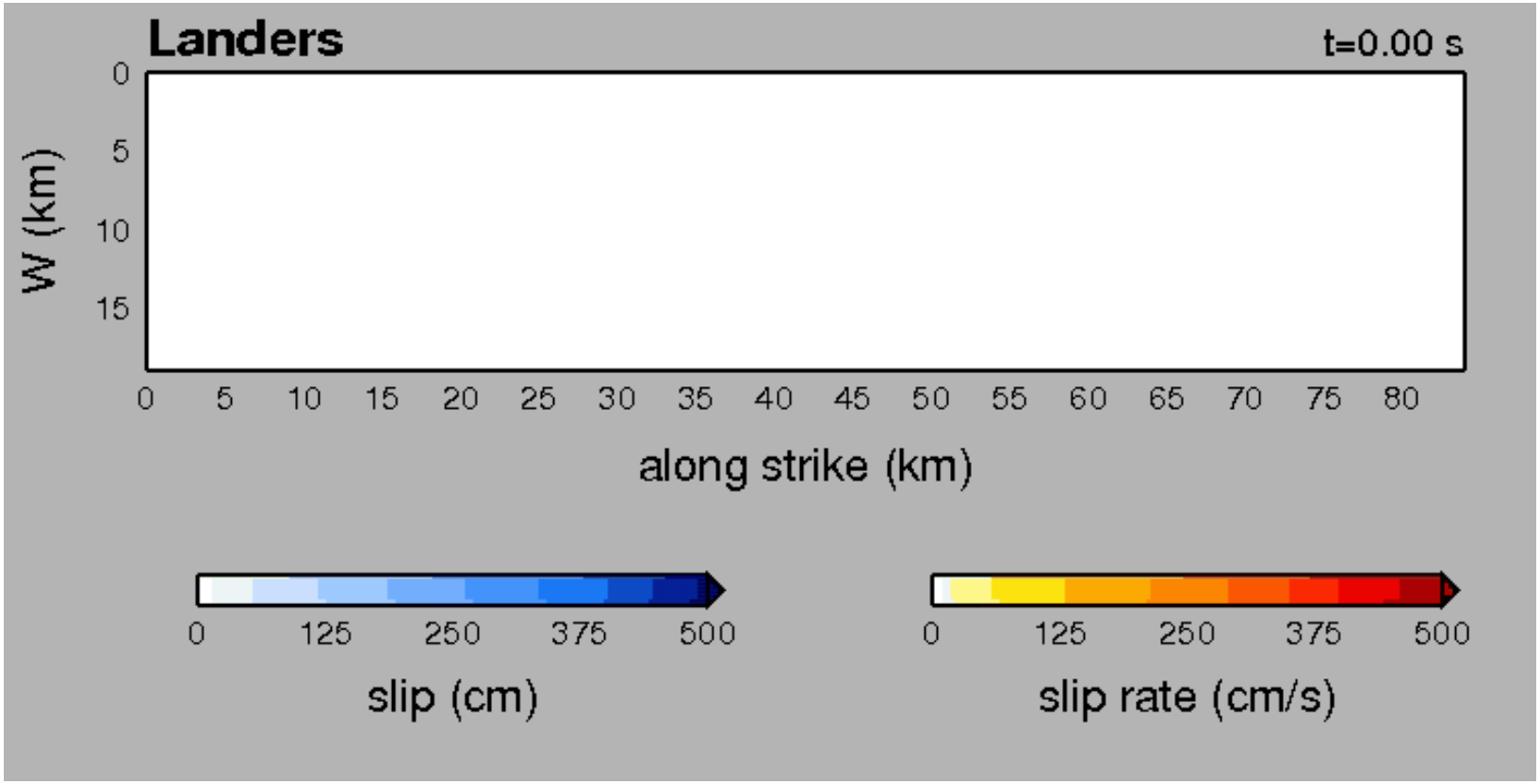

Low Frequency Representation Theorem

The low frequency simulation utilizes the basic representation theorem presented earlier

$$u_j(t) = S_{i=1,N}\, G_{ij}(t) * D_i(t)$$

where the $D_i(t)$ are given by the rupture characterization described in the previous section and the $G_{ij}(t)$ are Green's functions (GFs) describing wave propagation from the i^{th} subfault to the j^{th} receiver.

The current implementation of the Broadband Platform is restricted to 1D velocity structures. The use of 1D media allows for very efficient use and storage of the GFs.

In our implementation, the GFs are computed using the frequency-wavenumber (FK) technique of Zhu and Rivera (2002). The FK GFs contain the full theoretical waveform response from zero frequency to the upper limit specified in the calculation (typically several Hz). The Zhu and Rivera method computes GFs for 3 fundamental fault orientations, from which any arbitrary faulting mechanism can be computed using a linear combination of the fundamental fault responses.

The FK computation itself is not currently installed on the BBP. For the GP method, we pre-compute a database of GFs for a specified 1D velocity model and then this GF database is installed on the BBP.

For efficiency, the GFs are computed for a matrix of depths and distances covering the anticipated range of these parameters that might be encountered in the simulations. For WUS GFs, the depth range is 0-30 km and the distance range is 0-500 km. For ENA, the depth range is 0-35 km and the distance range is 0-1100 km.

Green's Functions Table

The listing below shows the distances (1st block) and depths (2nd block) for a set of pre-computed WUS GFs.

Note that the sampling is not constant. It is finer at close distance and near the surface, and then increases with increasing distance and depth.

```
140
    0.1000    0.2000    0.4000    0.6000    0.8000    1.0000
    2.0000    3.0000    4.0000    5.0000    6.0000    7.0000
    8.0000    9.0000   10.0000   11.0000   12.0000   13.0000
   14.0000   15.0000   16.0000   17.0000   18.0000   19.0000
   20.0000   22.0000   24.0000   26.0000   28.0000   30.0000
   32.0000   34.0000   36.0000   38.0000   40.0000   42.0000
   44.0000   46.0000   48.0000   50.0000   52.0000   54.0000
   56.0000   58.0000   60.0000   64.0000   68.0000   72.0000
        .
        .
        .
  465.0000  470.0000  475.0000  480.0000  485.0000  490.0000
  495.0000  500.0000
50
    0.1000    0.2000    0.4000    0.6000    0.8000    1.0000
    1.2500    1.5000    1.7500    2.0000    2.2500    2.5000
    2.7500    3.0000    3.2500    3.5000    3.7500    4.0000
    4.5000    5.0000    5.5000    6.0000    6.5000    7.0000
    7.5000    8.0000    8.5000    9.0000    9.5000   10.0000
   11.0000   12.0000   13.0000   14.0000   15.0000   16.0000
   17.0000   18.0000   19.0000   20.0000   21.0000   22.0000
   23.0000   24.0000   25.0000   26.0000   27.0000   28.0000
   29.0000   30.0000
```

distance block

depth block

Green's Functions Interpolation

For each station in the LF simulation, the code loops over all the subfaults sequentially and sums the individual responses to obtain the total response. The GFs needed for each subfault are determined by the depth of the subfault and the distance from the subfault to the station, denoted here by d_E and r_E.

The code then looks up in the table to find the 2 closest depths and distances that bracket the desired location, i.e.,

$$d_m \le d_E \le d_p$$

$$r_m \le r_E \le r_p$$

If there is an exact match to both the depth and distance, then that GF is selected and used in the simulation.

If an exact match is not found, then interpolation is done using weights given by the inverse distance to the exact point and by applying time shifts to align the S arrival.

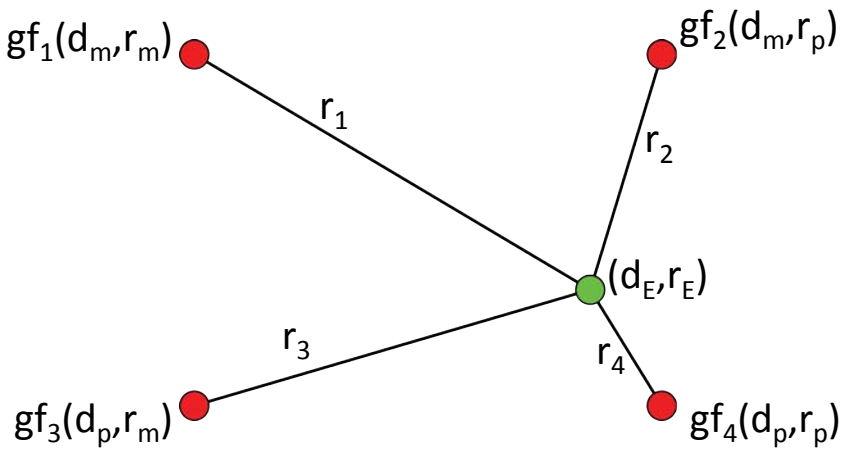

$$gf_E(t) \approx \sum_{i=1,4} gf_i(t-Dt_i)\, w_i$$

$$w_i = (1.0/r_i)\left[\sum_{i=1,4} 1/r_i\right]^{-1}$$

High Frequency Representation Theorem

The high frequency simulation approach is based on the "stochastic" method first introduced for point sources by Boore (1993). The extension to finite-faults is described by Frankel (1995), Beresnev and Atkinson (1997) , and Hartzell et al. (1999), among many others. The representation is constructed in the frequency domain and aims to match the w^2 amplitude spectrum as described by Brune (1970).

Denoting A(f) as the Fourier transform of the ground acceleration waveform a(t) observed at a particular site for a specified fault rupture, this can then be represented as the summation of the individual responses $A_i(f)$ from each subfault, where N is the total number of subfaults.

$$\mathcal{F}\{a(t)\} = A(f) = \sum_{i=1,N} A_i(f)$$

The acceleration spectrum for the i^{th} subfault is given by

$$A_i(f) = \sum_{j=1,M} C_{ij}\, S_i(f)\, G_{ij}(f)\, P(f)\, W_i^*(f)$$

where the summation j=1,M accounts for different possible ray paths (e.g., direct, Moho-reflected), and

C_{ij}	radiation scale factor
$S_i(f)$	subfault source amplitude spectrum
$G_{ij}(f)$	path term
$P(f)$	site attenuation term
$W_i^*(f)$	complex spectrum of windowed time series

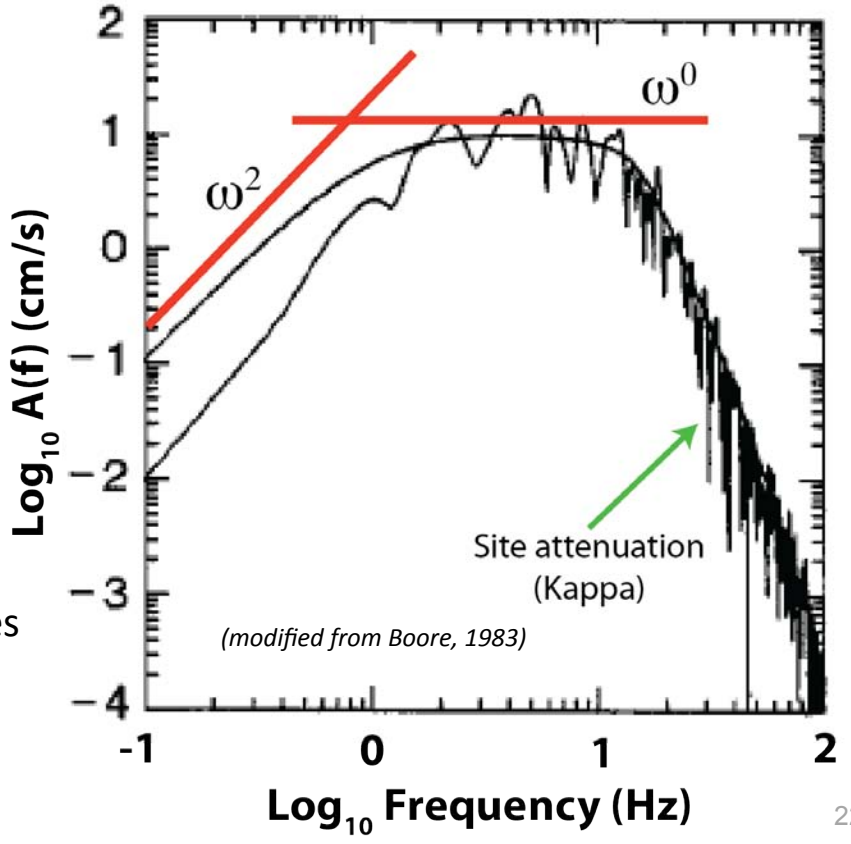

Radiation Scale Factor C_{ij}

$$A_i(f) = S_{j=1,M}\, C_{ij}\, S_i(f)\, G_{ij}(f)\, P(f)\, W_i^*(f)$$

The radiation scale factor is given by

$$C_{ij} = F_s\, R_{Pij} / (4\, p\, r_i\, b_i^3)$$

which represents the radiation for far-field S waves (Aki and Richards, 1980).

F_s = 2 accounts for free surface amplification (assumes vertical incidence S-waves).

R_{Pij} is a conically averaged radiation pattern term spanning a range of ±45° in slip mechanism and take-off angle for the j^{th} ray.

r_i and b_i are the density and shear-wave velocity at the center of the i^{th} subfault.

Subfault Source Amplitude Spectrum $S_i(f)$

$$A_i(f) = S_{j=1,M}\, C_{ij}\, S_i(f)\, G_{ij}(f)\, P(f)\, W_i^*(f)$$

The subfault source amplitude spectrum is given by

$$S_i(f) = m_i\, f^2\, [1 + F \cdot f^2 / f_{ci}^2]^{-1}$$

which represents the w^2 source radiation.

$m_i = d_i\, m_i\, a_i$ is the seismic moment release of the i^{th} subfault with d_i, m_i, a_i being the slip, rigidity and area of the i^{th} subfault.

$f_{ci} = c_0\, V_{Ri} / (a_T\, p\, dl)$ is the subfault (subevent) corner frequency with V_{Ri} the local rupture speed (including shallow weak zone) and c_0 is set to 2.0 for WUS and 1.32 for ENA.

$F = M_o / (N\, s_p\, dl^3)$ is a factor introduced by Frankel (1995), which scales the subfault corner frequency to that of the mainshock and ensures the total moment of the summed subfaults is the same as the mainshock moment M_o. N is the total number of subfaults, s_p is the Brune stress parameter (set 50 bars for WUS, 100 bars for ENA), and dl is the average subfault dimension.

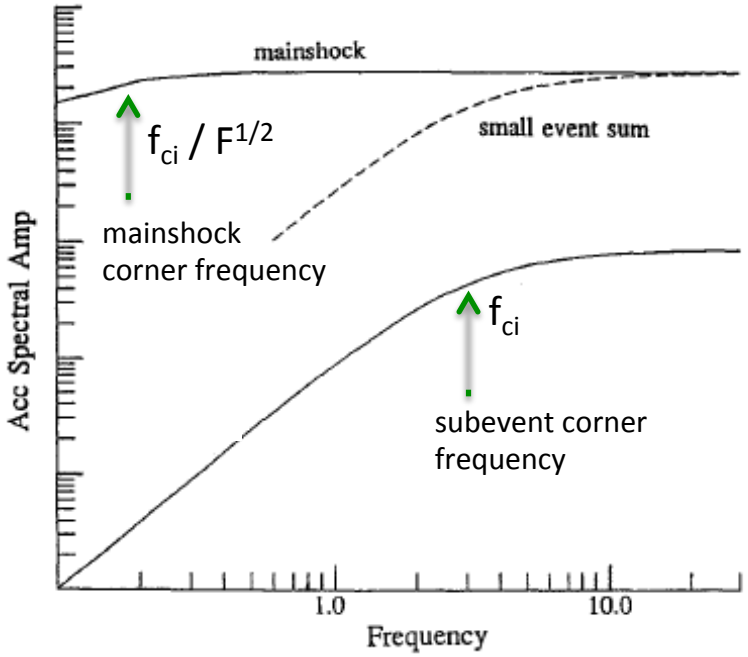

Path Term $G_{ij}(f)$

$$A_i(f) = S_{j=1,M}\, C_{ij}\, S_i(f)\, G_{ij}(f)\, P(f)\, W_i^*(f)$$

The path term is given by

$$G_{ij}(f) = \{I_i(f) / r_{ij}\} \exp\{-p\, f^{1-x}\, S_{k=1,L}\, t_{ijk}/q_k\}$$

which represents impedance, geometric spreading and attenuation effects along the propagation path.

$I_i(f)$ represents gross impedance effects from the i^{th} subfault to the ground surface computed using quarter wavelength theory for the prescribed 1D velocity structure (Boore and Joyner, 1997).

r_{ij} is the total path length of the j^{th} ray from the i^{th} subfault to the receiver.

exp{□} models anelasticity and scattering via a travel-time weighted average of the Q values for each of the velocity layers (Ou and Herrmann, 1990). The assumed frequency dependence is of the form $Q(f)=Q_0 f^x$. The summation over k=1,L represents all of the ray path segments through the layers of the 1D velocity model, with t_{ijk} and q_k being the travel-time of the particular ray segment and Q value, respectively, within each velocity layer k.

WUS: x=0.6, $Q_0 \approx 120$
ENA: x=0.45, $Q_0 \approx 500$

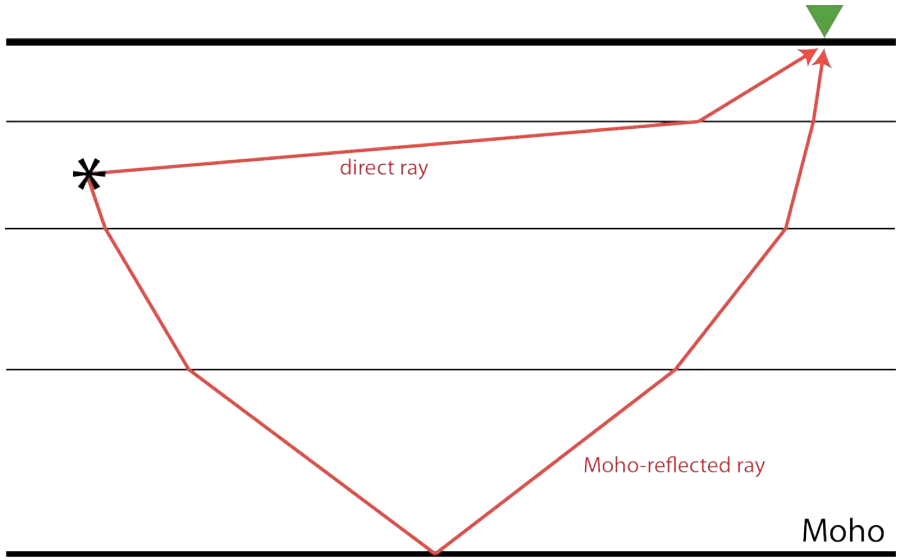

USGS science for a changing world

Site Attenuation Term P(f)

$$A_i(f) = S_{j=1,M}\, C_{ij}\, S_i(f)\, G_{ij}(f)\, P(f)\, W_i^*(f)$$

The site attenuation term is given by

$$P(f) = \exp[-p\, k_0\, f]$$

which models near site high-frequency spectral decay based on the Kappa model introduced by Anderson and Hough (1984). We set $k_0 = 0.04$ for WUS and $k_0 = 0.015$ for ENA.

Complex Spectrum of Windowed Time Series $W_i^*(f)$

$$A_i(f) = S_{j=1,M}\, C_{ij}\, S_i(f)\, G_{ij}(f)\, P(f)\, W_i^*(f)$$

This term incorporates **all of the phasing** information for the high frequency simulation.

Following Boore (1983) it is derived by first taking a windowed time sequence of band-limited random white Gaussian noise (*"stochastic"*) and normalizing to have zero mean and scaling the variance to have unit spectral amplitude on average.

Our implementation uses the envelope function from Saragoni and Hart (1974) to shape the time sequence and set the peak of the envelope at the direct S-wave arrival time.

The duration of the windowed time sequence for the i^{th} subfault is given by

$$T_{di} = f_{ci}^{-1} + c_T\, r_{ij}$$

where c_T is set to 0.07 for WUS and 0.1 for ENA.

This term also incorporates the time delay for rupture propagation across the fault as well as the travel time for the particular ray being considered.

Once constructed in the time domain, this term is transformed into a complex valued frequency domain function that is then combined with the other amplitude shaping terms.

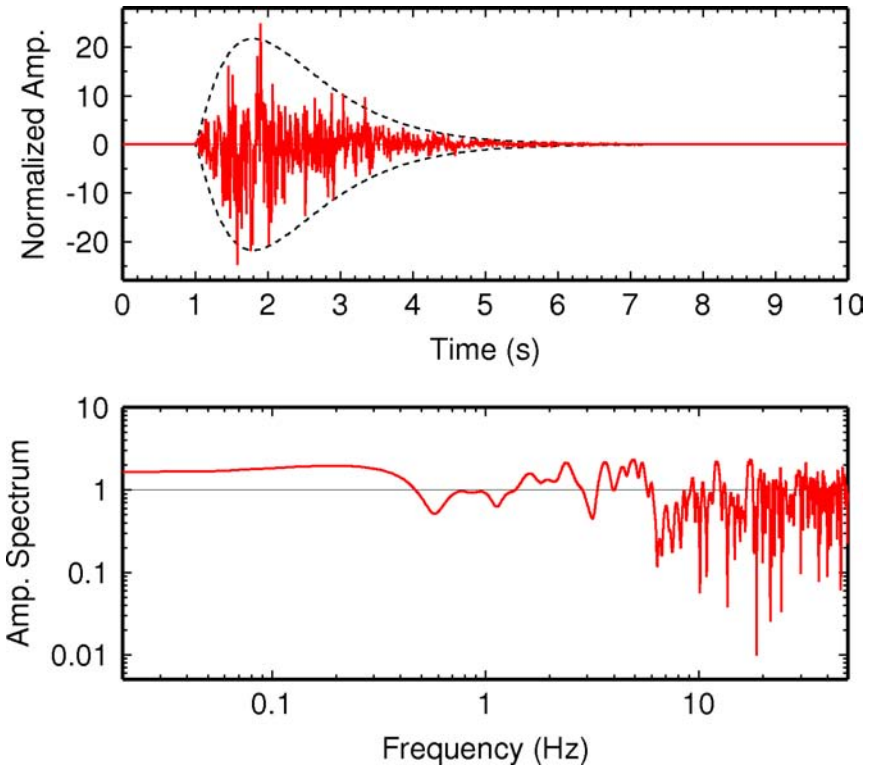

What does the Stochastic Phasing of $W_i^*(f)$ Represent?

The stochastic simulation approach, as originally developed by Hanks and McGuire (1981) and Boore (1983), was designed to match the statistical properties of observed high frequency ground motions using a simple, far-field model of the radiated amplitude spectra.

In this model, the stochastic phasing represents the **unmodeled details** of both the rupture process and scattering effects along the propagation path. Thus, there is no explicit slip-rate function in this approach and all of the detailed phasing effects from rupture across a subfault are incorporated stochastically within $W_i^*(f)$.

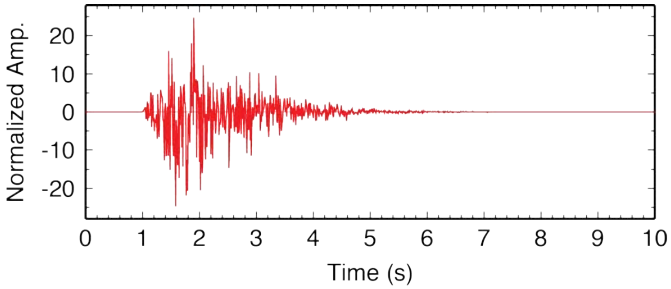

Since these features are represented stochastically, we do not require the fine spatial and temporal resolution of the kinematic rupture described earlier. In our HF implementation, we downsample the rupture to subfaults with dimensions of 1-2 km. We find 2 km X 2 km subfaults work well for WUS, and 1 km X 1 km work well for ENA (slight adjustments allowed to match overall fault dimensions).

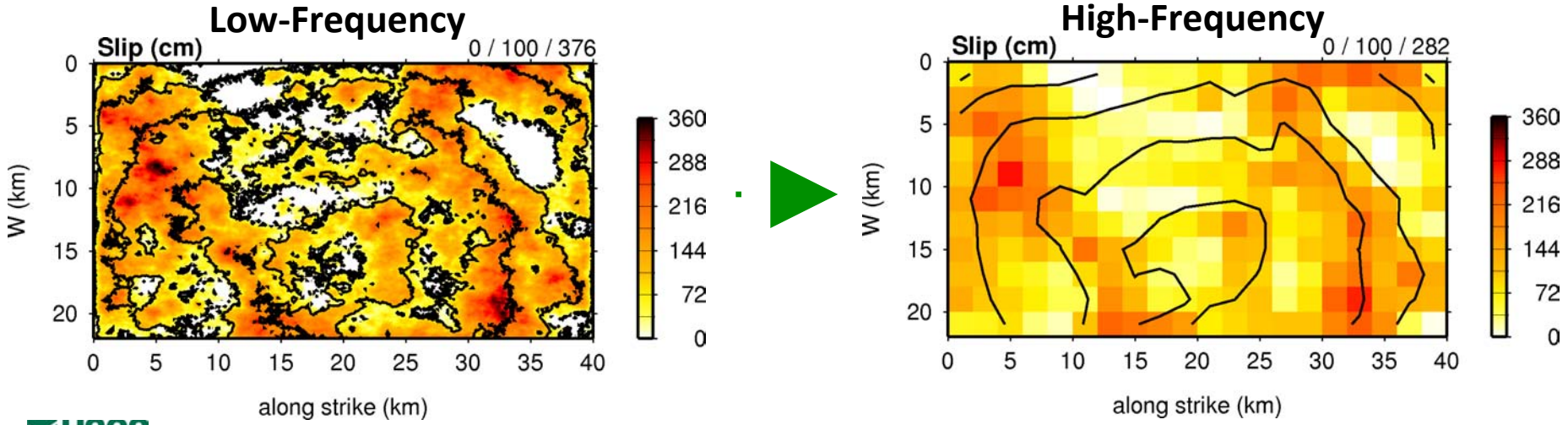

Combining the Low- and High-Frequency Responses

Match Filtering

All hybrid simulation methods use some process of filtering and summation to combine the separate low- and high-frequency responses into a full broadband time series. There are a variety of approaches for this, each with its advantages and drawbacks. The basic assumption of all approaches is that the amplitude and phasing of the individual LF and HF responses are compatible across the cross-over frequency.

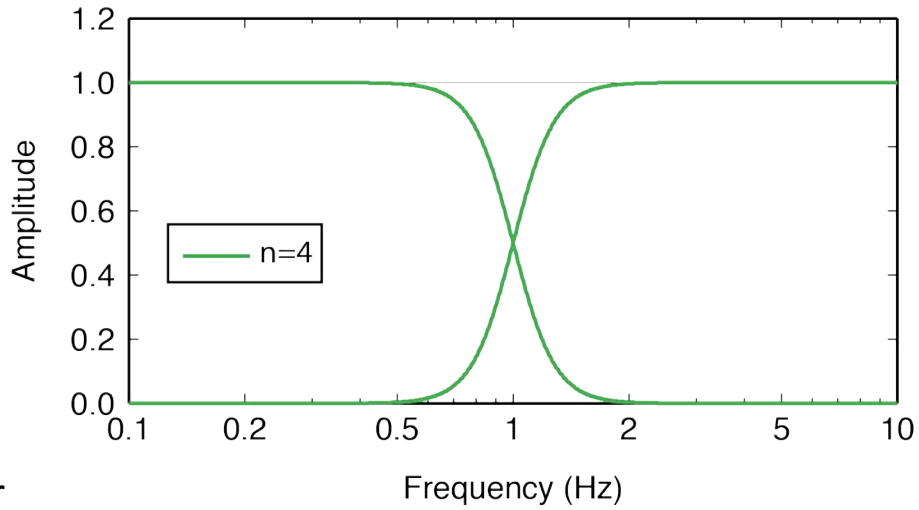

In our implementation, we use a set of "matched" 4th order zero-phase Butterworth filters each with a corner frequency at f_m=1 Hz. A high-pass filter is applied to the HF response, and a low-pass filter is applied to the LF response. The filters sum to unity across all frequencies.

$$LP(f) = [1 + (f/f_m)^{2n}]^{-1} \qquad HP(f) = [1 + (f_m/f)^{2n}]^{-1}$$

The filtering is done in the time domain and the broadband response is obtained by summing the filtered results:

$$a_{BB}(t) = lp(t)*a_{LF}(t) + hp(t)*a_{HF}(t)$$

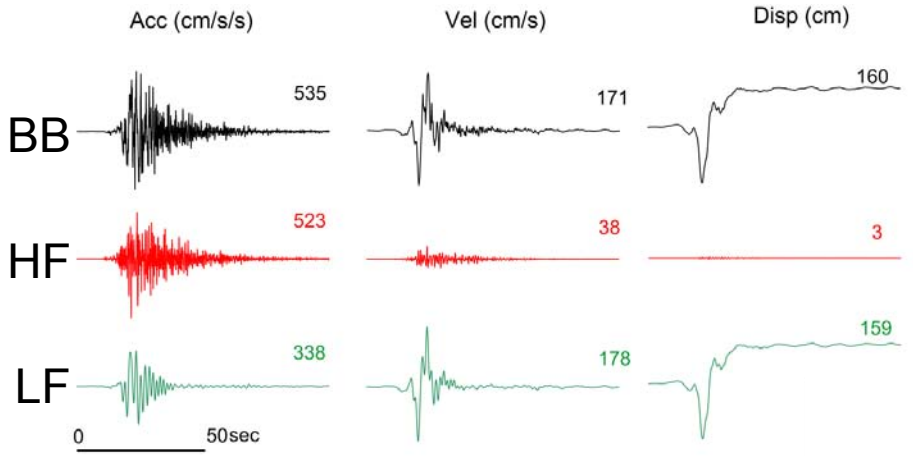

Combining the Low- and High-Frequency Responses

Some Caveats on Combining Hybrid Simulations

Generally, the separate low- and high-frequency simulations will not be exactly compatible around the cross-over frequency. In particular, any differences in phasing will cause a reduction of the summed amplitude response near the cross-over frequency.

This occurs because the combination is a vector summation over both amplitude and phase. Any difference in phase between the LF and HF portions will act to reduce the combined BB amplitude.

$$|V_{BB}| \leq |V_{LF}| + |V_{HF}|$$

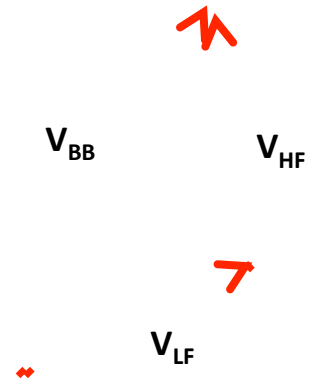

The only case where the amplitude of the sum is not reduced is when the phase of the LF and HF portions are identical (which does not generally occur).

One way to minimize the impact of this effect is to make the filters as sharp as possible, for example, by increasing the order of the Butterworth operators. This doesn't eliminate the effect, but it concentrates it into a narrow frequency band.

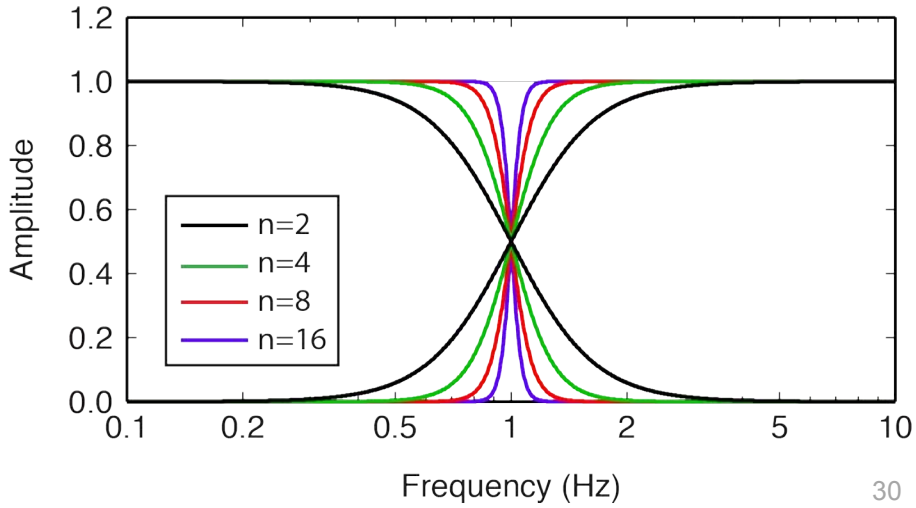

Combining the Low- and High-Frequency Responses

But Beware!

What might appear to work well in the frequency domain might not do so well in the time domain (and vice-versa).

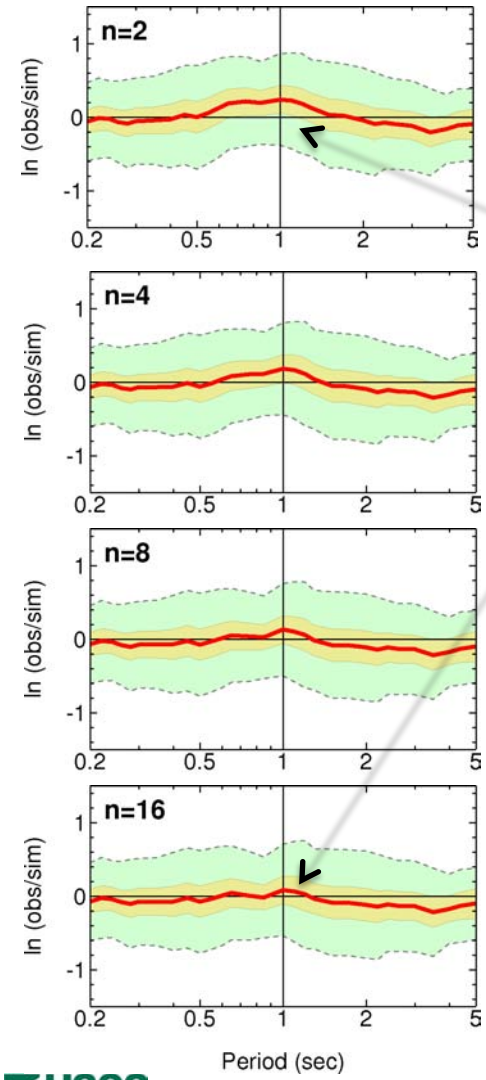

Increasing the sharpness of the filters does reduce the significance of the under-prediction in the spectral domain.

But comes at the expense of introducing acausal artifacts in the time domain.

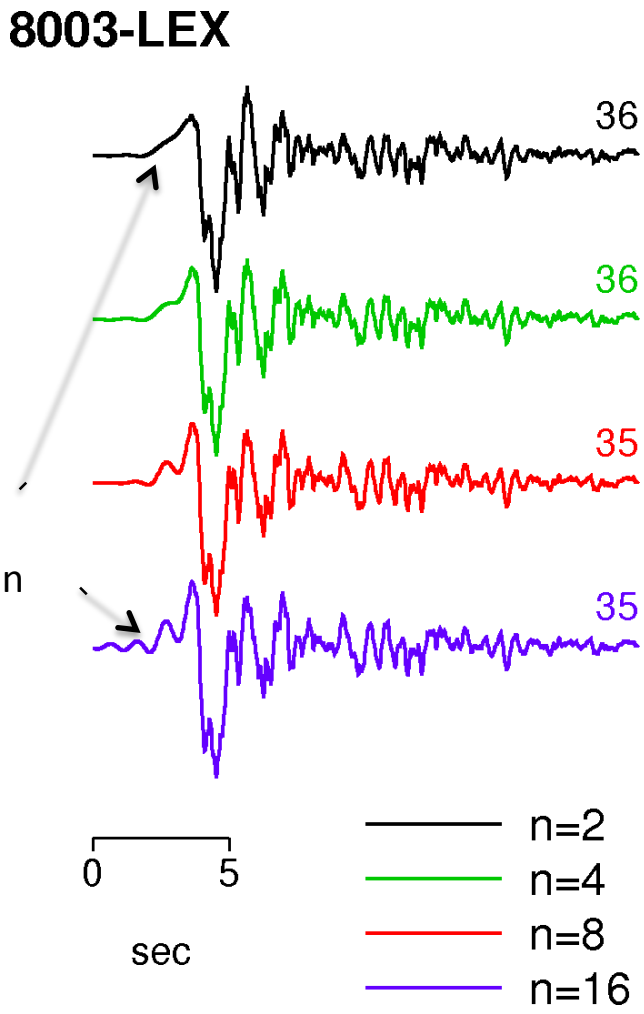

Research Needs

- Improve kinematic rupture characterization with guidance from rupture dynamics
- Improve models of non-linear response, both near fault and near surface
- Push "low-frequency" approach to higher frequencies

  - **Ultimate goal is to eliminate need for "hybrid" approach; that is, develop a unified approach applicable to broad frequency range**

Hidden Parameters

The current configuration of the BBP allows the user to specify some general parameters describing the source, station locations and Green's function. However, many of the underlying codes can accept a number of parameters that can be changed in the simulations. These parameters are "hidden" in the sense they cannot be changed using the standard BBP interface.

Modifying these parameters requires editing the python scripts that form the basis of the BBP workflow. Time permitting, this process will be discussed during the afternoon exercises.

For example, some of the relevant parameters in the GP method that a curious user might be interested in adjusting are:

Rupture Characterization:

`rvfrac`	-specifies the background rupture speed as a fraction of local V_s (0.8 WUS, 0.85 ENA)
`risetime_coef`	-gives the scaling of average risetime with seismic moment (1.45 WUS, 2.20 ENA)

High Frequency Simulation:

RVFAC	-specifies the background rupture speed as a fraction of local V_s (0.8 WUS, 0.85 ENA)
EXTRA_FCFAC	-gives the scaling of average corner frequency (0.0 WUS, -0.34 ENA) ($f_c = f_{c0}$*[1 + EXTRA_FCFAC])

Example: 1992 Landers EQ

- Multi-segment jumps (rupture delay)
- Shallow rupture effects

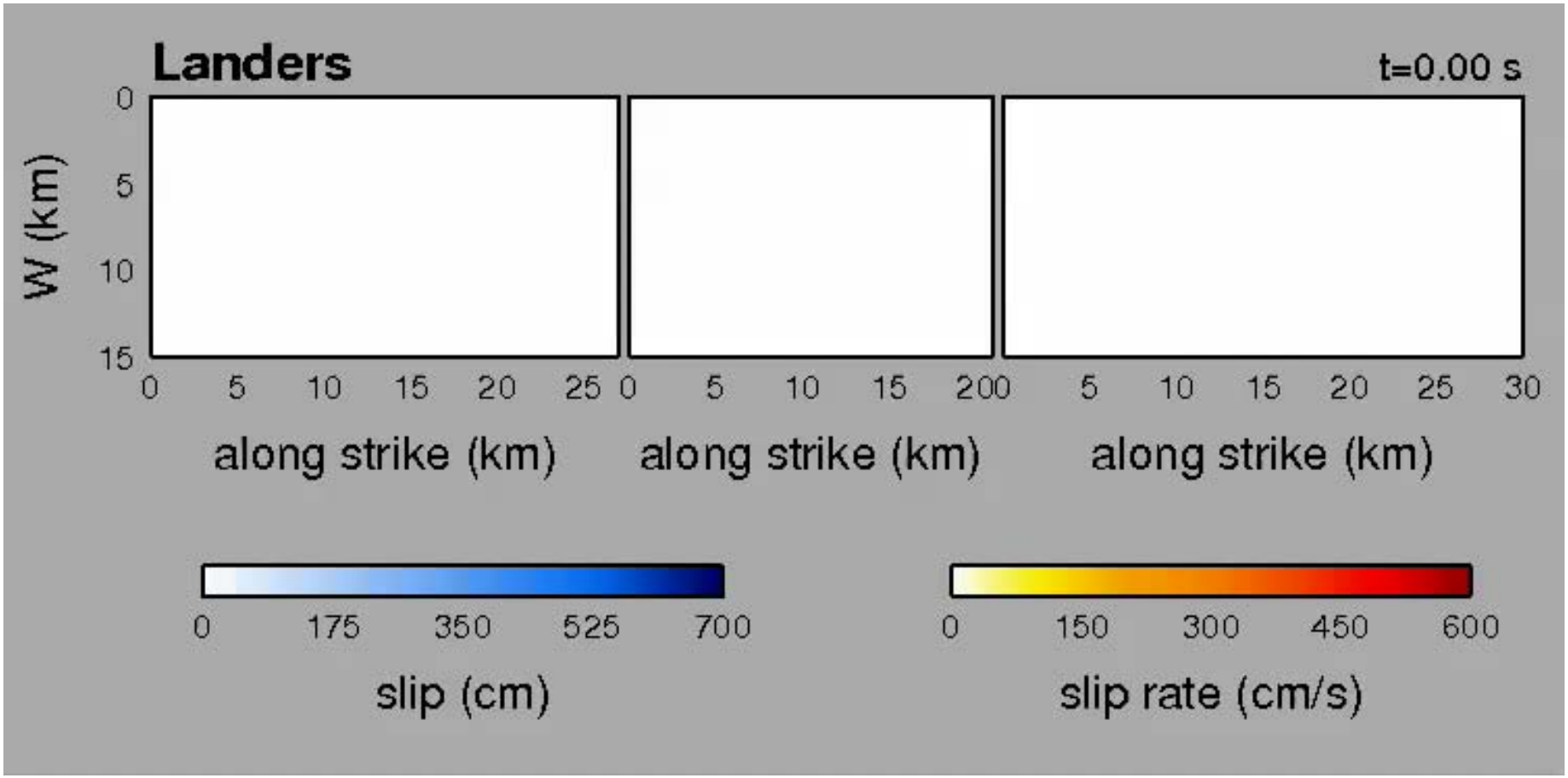

2. Rupture Initiation Time

First, compute background value T_B

$T_B = r_{path} / V_r$

V_r = 80% local V_s depth > 8 km

= 56% local V_s depth < 5 km

With a linear transition between 5-8 km

Reduction of V_r above 5 km depth for WUS represents velocity strengthening behavior in weaker near-surface material

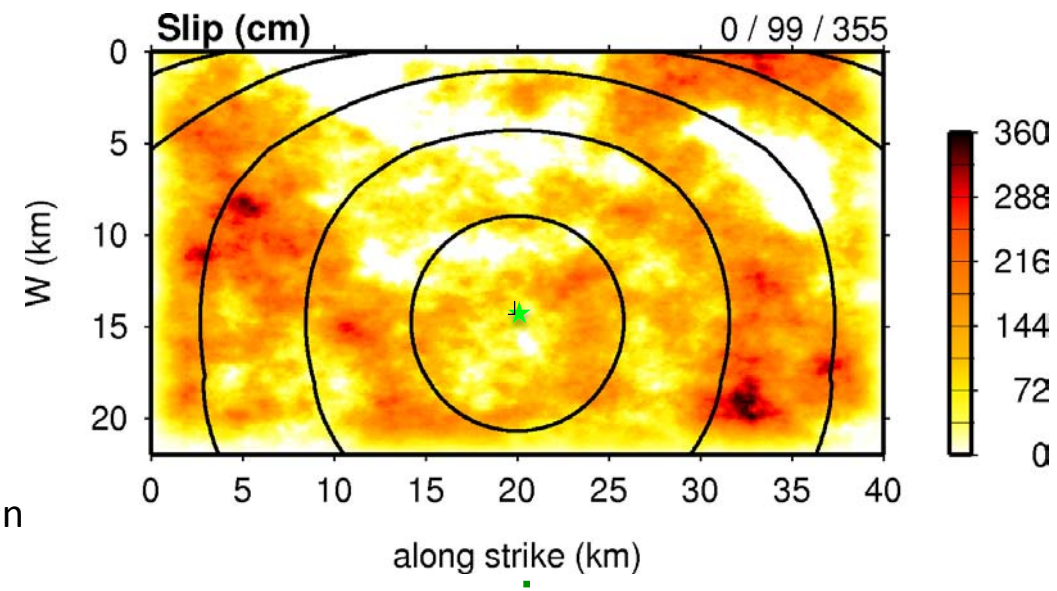

For M_w = 6.94

$Dt_0(D_{max})$ = 1.2 s

Next, add timing adjustment that correlates with local slip

$T_i = T_B - Dt_0(D_i)$

Dt_0 scales with slip amount of i^{th} subfault (D_i) to accelerate or decelerate rupture

$Dt_0(D_{avg}) = 0$

$Dt_0(D_{max}) = 1.8 \times 10^{-9} \cdot M_o^{1/3}$

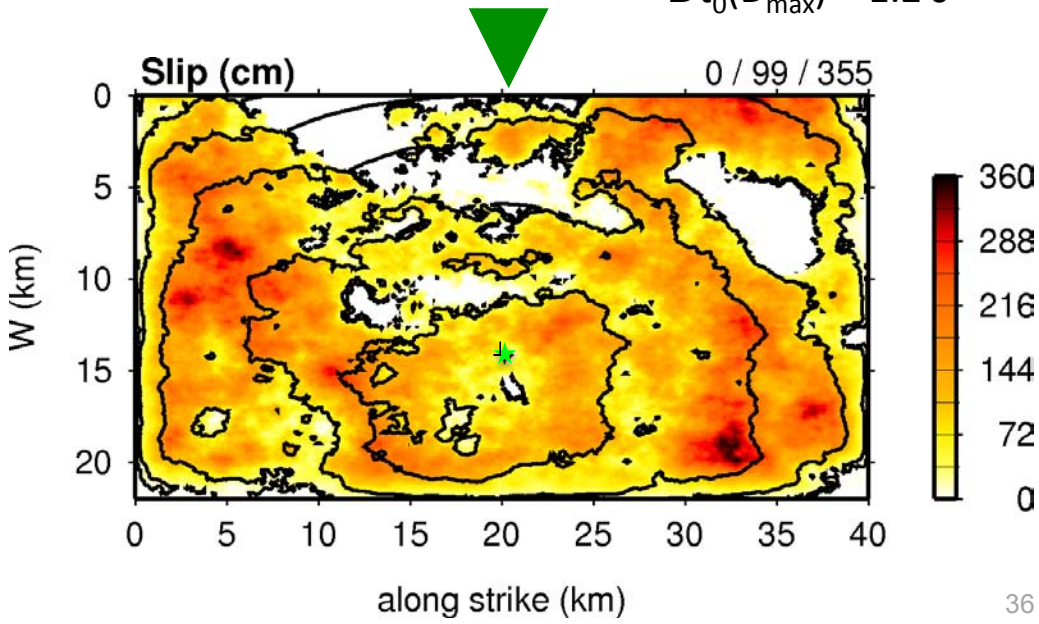

3. Slip Rate Function

Subfault rise time (t_i) scales with square root of local slip (D_i)

$t_i = k \cdot D_i^{1/2}$ depth > 8 km

$= 2 \cdot k \cdot D_i^{1/2}$ depth < 5 km (WUS only)

With a linear transition between 5-8 km

Lengthening of t_i above 5 km depth in WUS represents velocity strengthening behavior in weaker near-surface material

The constant (k) set so average rise time across entire fault is given by the relation:

$t_A = a_T \cdot c_1 \times 10^{-9} \cdot M_o^{1/3}$

where c_1=1.45 in WUS and 2.20 in ENA, and a_T is a mechanism dependent scaling factor (next slide).

The scaling with square root of slip represents a balance between constant rise time at one extreme and constant slip-rate at the other.

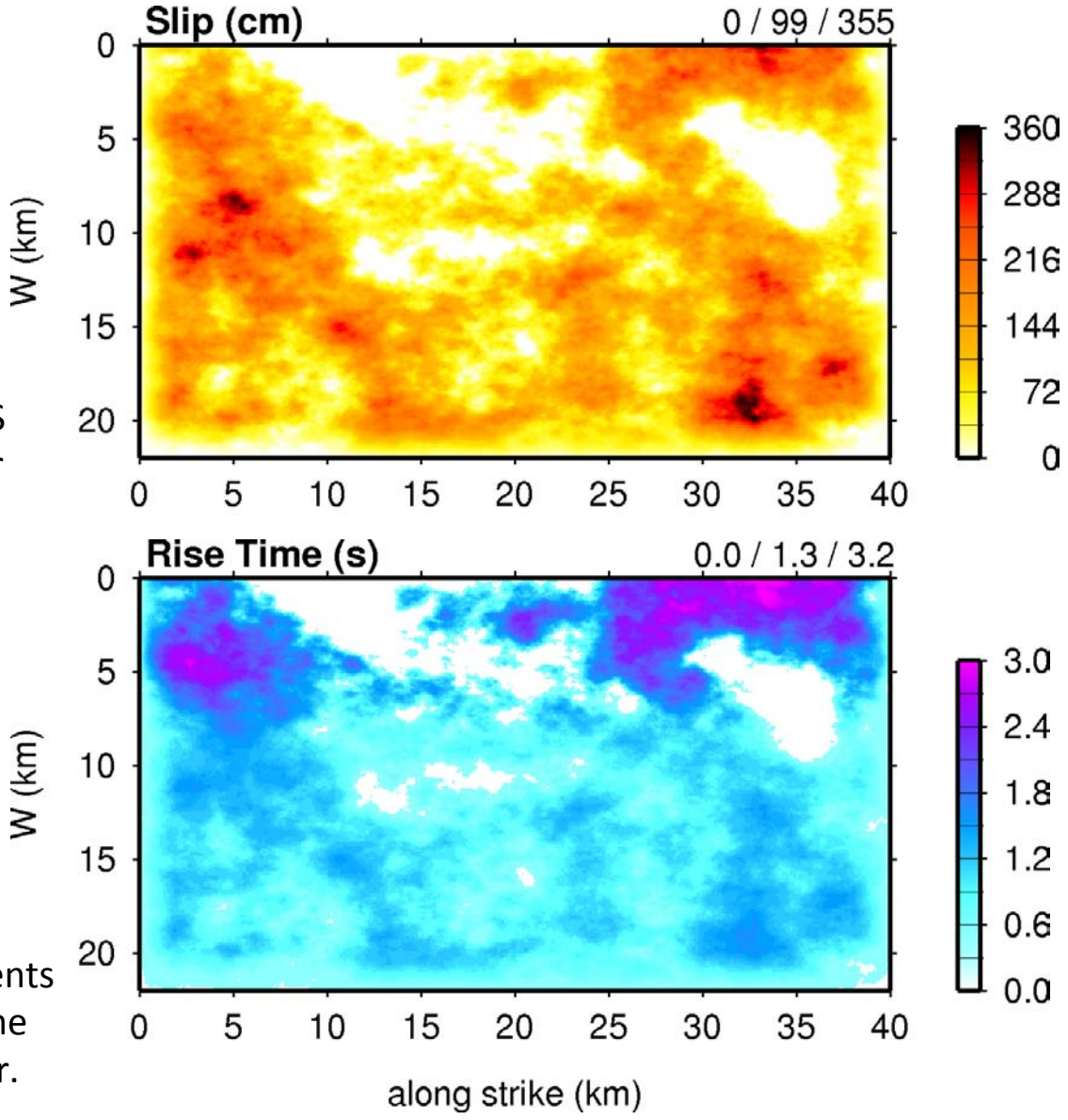

Low Frequency Simulation Methodology (f < 1 Hz)

- Kinematic representation of heterogeneous rupture on a finite fault
  - Heterogenous slip and rake
  - Rupture initiation time
  - Deterministic slip-rate function
- Visco-elastic wave propagation
  - 3D FD forward simulation
  - 1D FK using table of pre-computed Green's functions
- Site-specific non-linear amplification factors based on V_{s30}

High Frequency Simulation Methodology (f > 1 Hz)

- Limited kinematic representation of finite-fault rupture (extension of Boore, 1983)
  - Heterogeneous slip
  - Averaged radiation pattern
  - Rupture initiation time
  - Stochastic phase (represents unknown details of slip and scattering)
- Simplified Green's functions for 1D velocity structure
  - Separate GFs for direct and downgoing rays
  - Amplitude decays as inverse of ray path length
  - Gross impedance effects based on quarter wavelength (Boore and Joyner, 1997)
- Site-specific non-linear amplification factors based on V_{s30}

V_{s30} Based Amplification Functions for Large Scale Ground Motion Simulations

V_{s30} = travel-time averaged shear wave velocity in upper 30 meters

- Adopt V_{s30} site term from Campbell and Bozorgnia (2008) for use in simulations.
- Functions are frequency dependent and account for non-linear soil response
- Use of V_{s30} based approach is attractive
  - Readily available (or estimated)
  - Easy to compute and apply on large-scale

USGS science for a changing world

Motivation

- Large-scale EQ simulations produce ground motion waveforms at >100,000 sites, e.g. **ShakeOut**
- Incorporation of low velocity near surface material within the FD/FE simulation model can be extremely costly (prohibitive?) and requires special handling to account for soil non-linearity
- Need efficient site correction implementation scheme

ShakeOut: M_w 7.8 San Andreas Scenario

www.shakeout.org

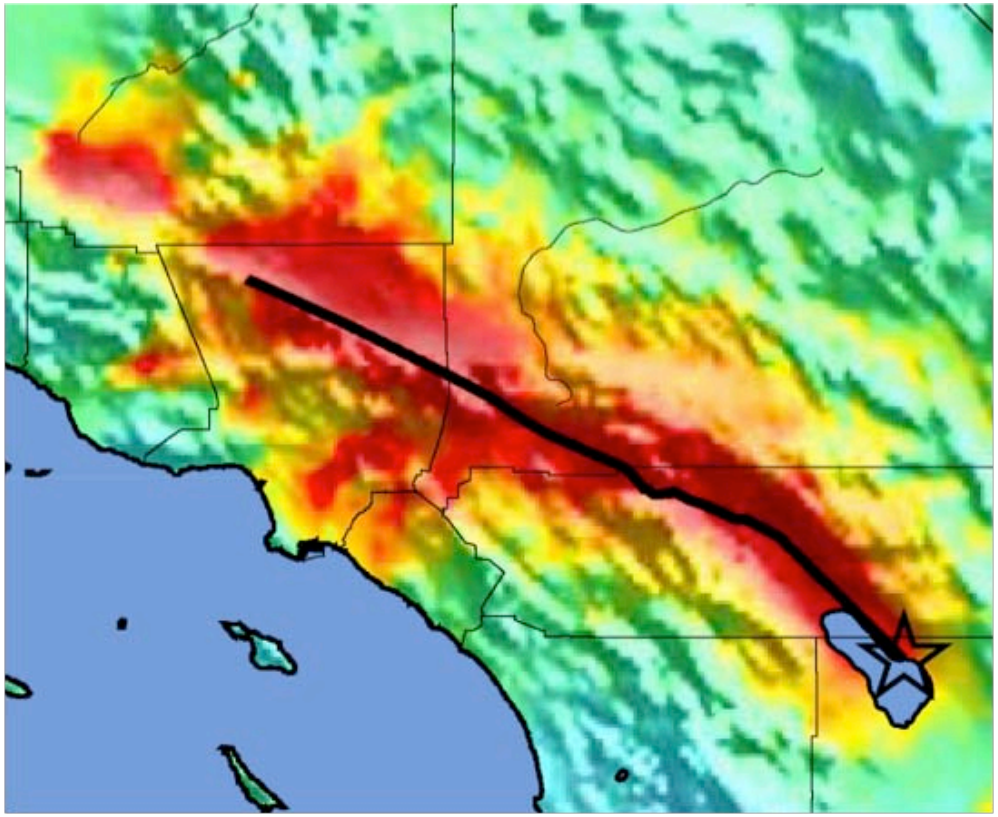

USGS science for a changing world

V_{s30} (measured or estimated) can easily be obtained for almost any region-

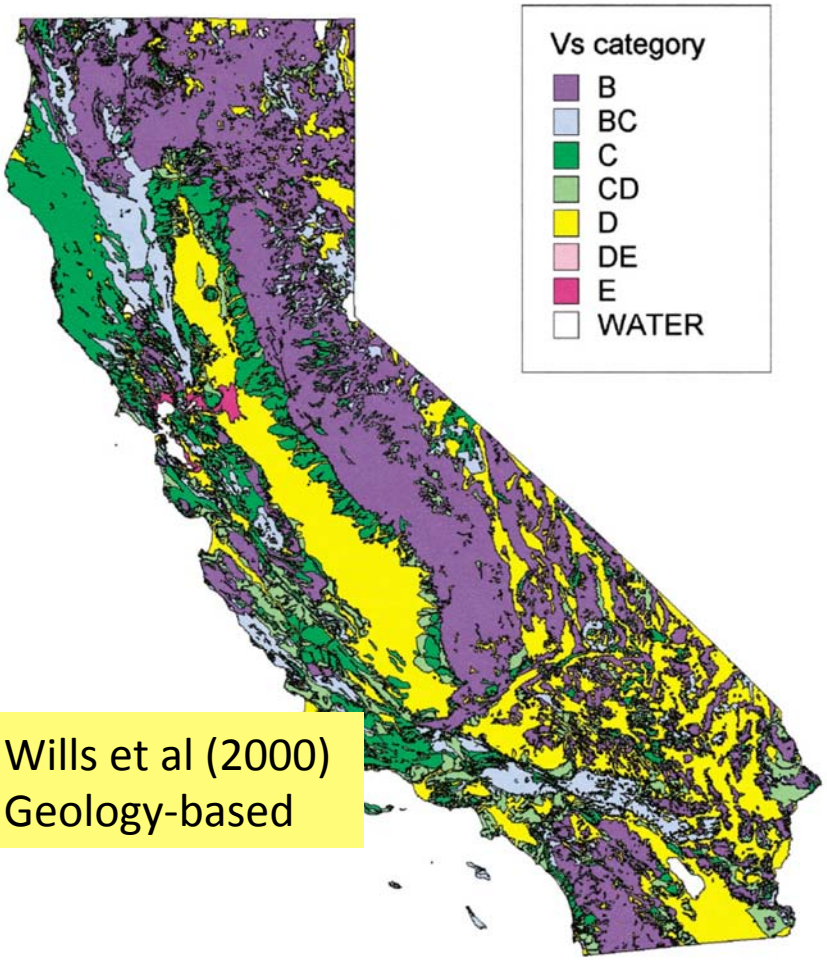

Wills et al (2000)
Geology-based

Yong et al. (2009)
Terrain-based

Wald and Allen (2007)
Topograhy-based

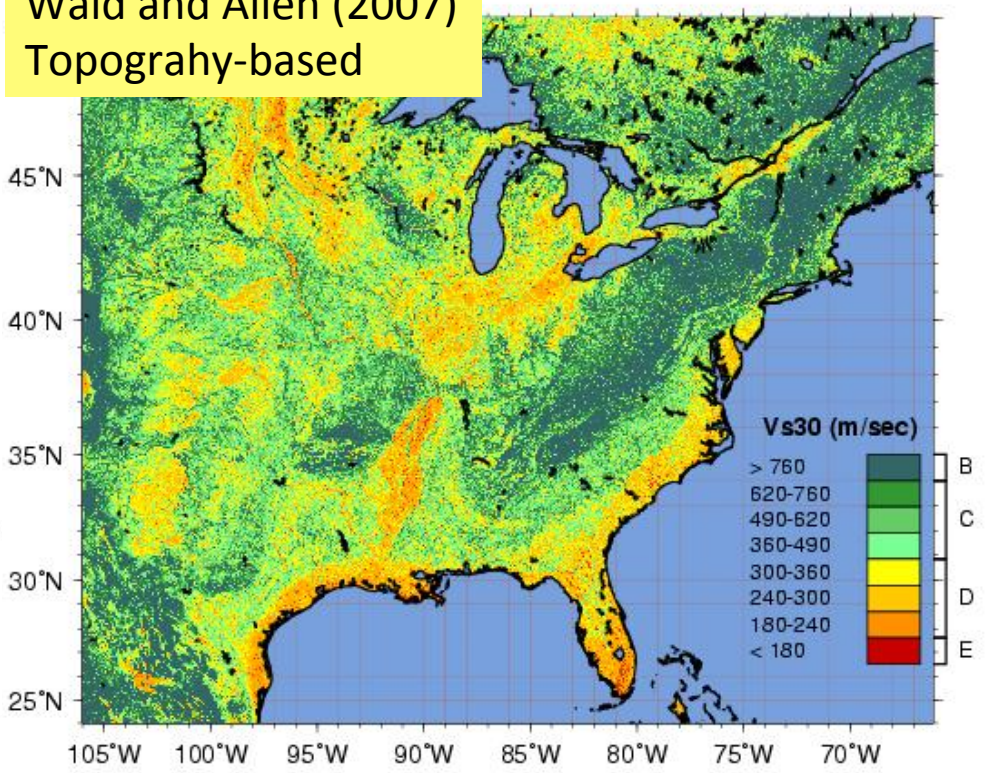

earthquake.usgs.gov/vs30

Amplification Function

- Based on equivalent linear response analysis (Walling et al., 2008) as implemented in the GMPE of Campbell and Bozorgnia (2008)
- Functional form:

$$\mathbf{A(f) = F_s(f,PGA_r,V_{site}) / F_s(f,PGA_r,V_{ref})}$$

where $F_s(f,PGA_r,V_{s30})$ = CB2008 site term

f = frequency (1/T)

PGA_r = input rock PGA (V_{s30} = 1100 m/s)

V_{ref} = V_{s30} used in simulation model

V_{site} = V_{s30} at site of interest

V_{site} Dependence

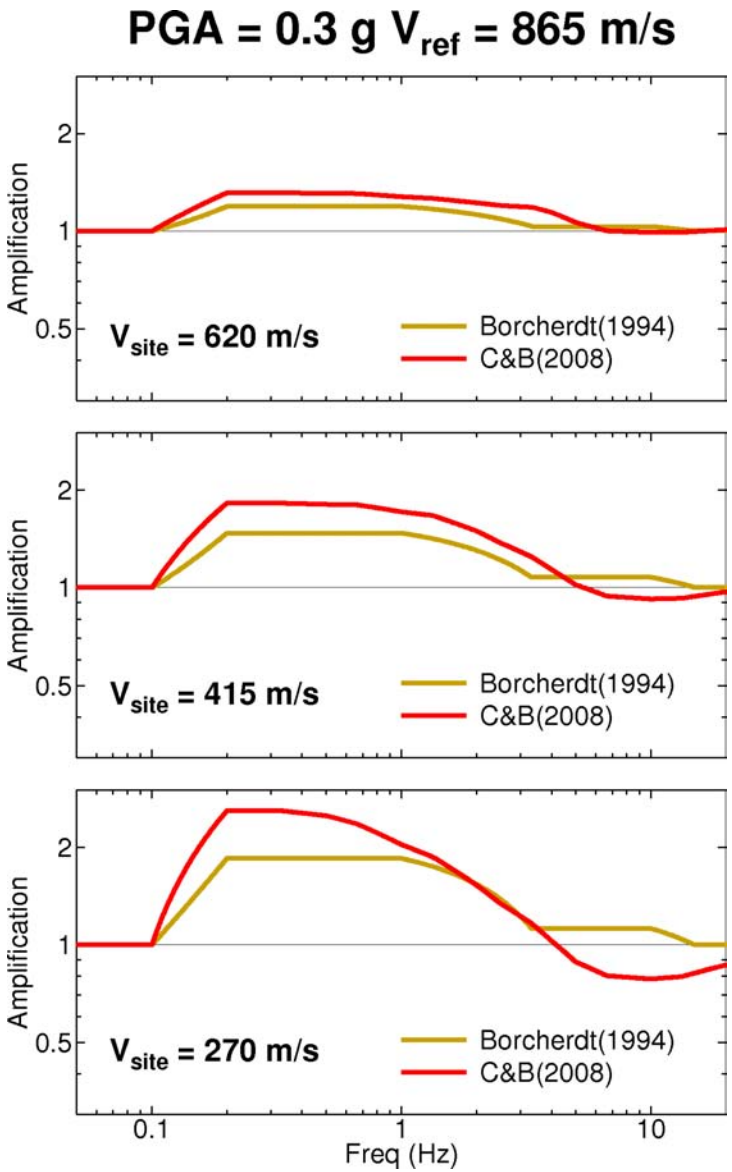

PGA_{rock} Dependence

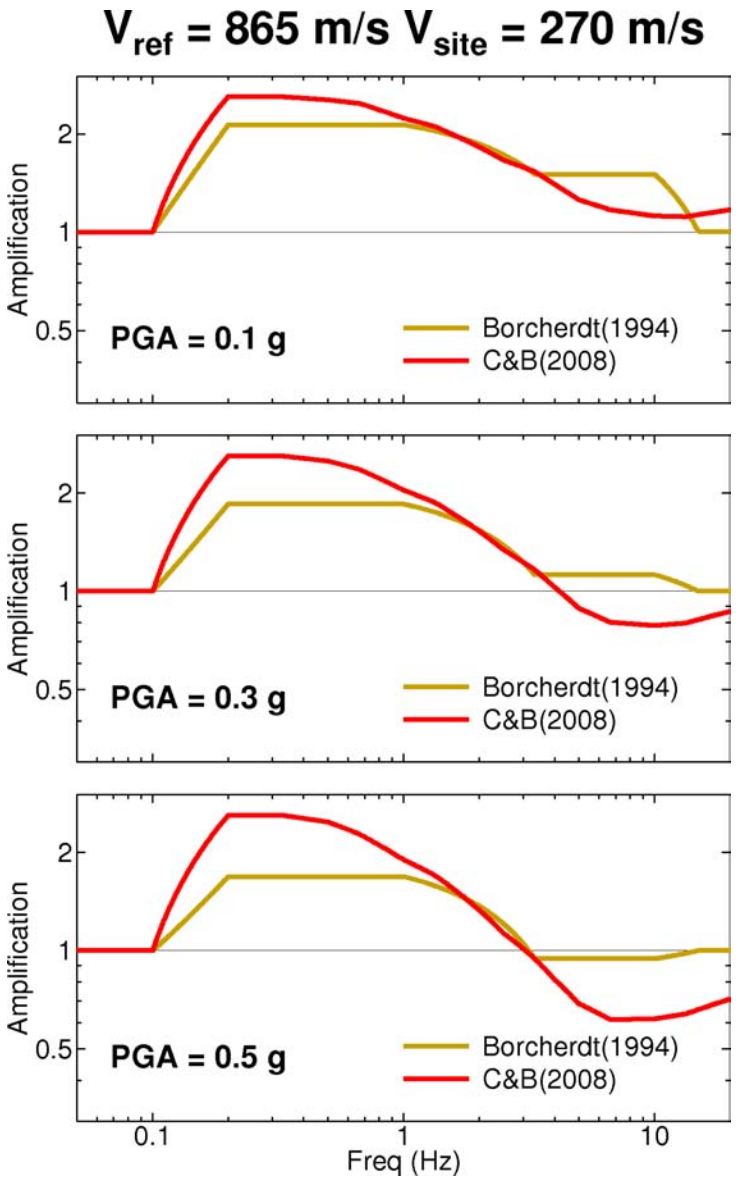

USGS science for a changing world

Time Series Implementation

- Construct amplitude spectrum given PGA_{rock}, V_{ref} and V_{site}.
- Fourier transform time series into frequency domain.
- Scale FAS by computed amplitude spectrum.
- Inverse transform back to time domain.

$g_{ref}(t)$: acceleration time series at V_{ref} → PGA_{rock}

$$G_{ref}(f) = F\{g_{ref}(t)\}$$

$$G_{site}(f) = A(f) \cdot G_{ref}(f)$$

$$g_{site}(t) = F^{-1}\{G_{site}(f)\}$$

USGS science for a changing world

Implementation Caveats

- Functions are defined for response spectra, but are applied to Fourier spectra. OK, as long as functions vary slowly with frequency.
- No phase modification
  - no multiples / reverberations
  - potential causality issues

Can be alleviated using wavelet-based spectral matching techniques, but at increased computational cost.

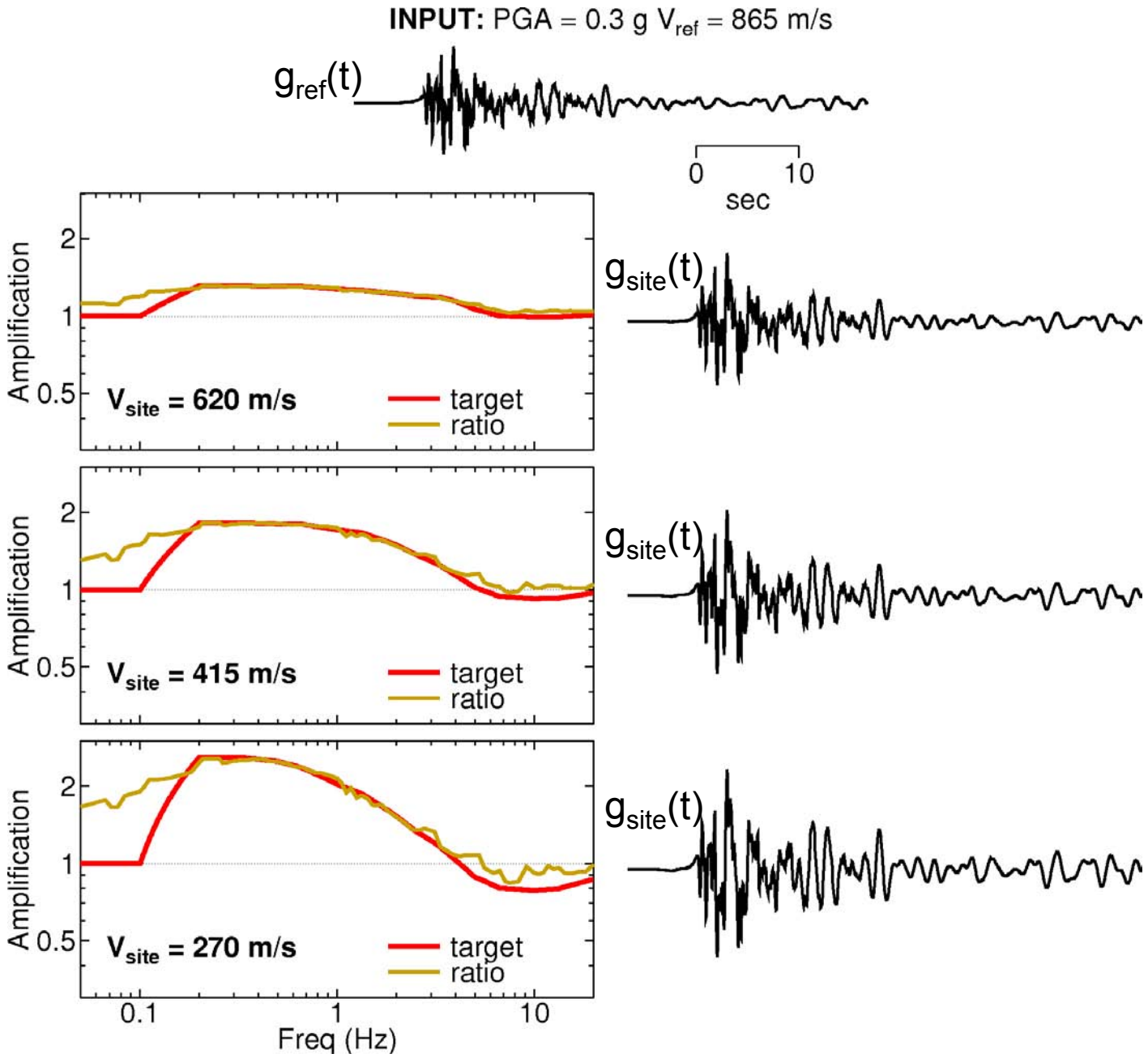
INPUT: PGA = 0.3 g V_{ref} = 865 m/s
$g_{ref}(t)$
0
10
sec
Amplification
2
1
0.5
V_{site} = 620 m/s
target
ratio
$g_{site}(t)$
V_{site} = 415 m/s
V_{site} = 270 m/s
0.1
1
10
Freq (Hz)

Example Application: 1994 Northridge Earthquake

Full Site Correction

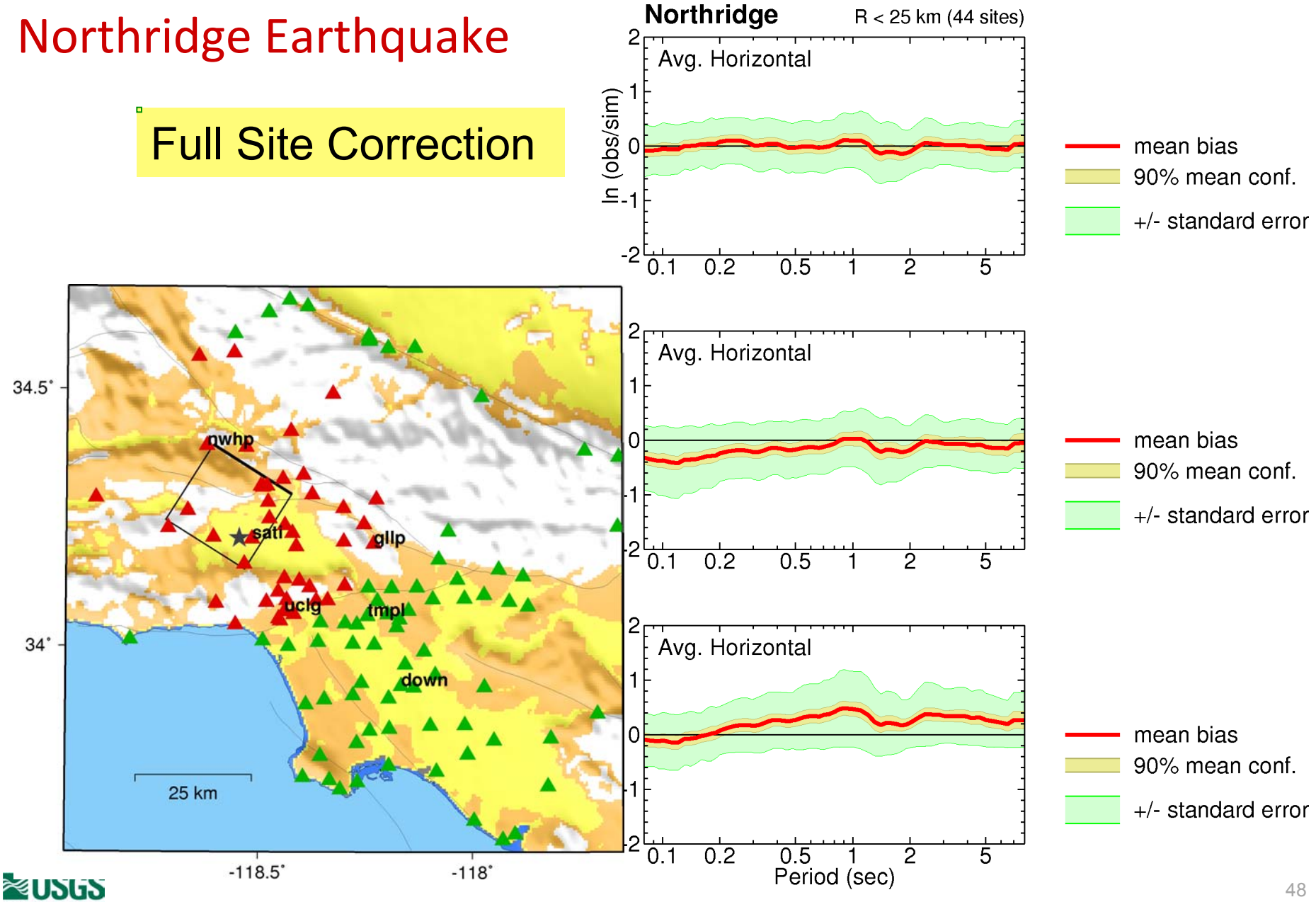

Vs30 Amplification Function Summary

- **Benefits**
  - Easy to implement on large scale
  - Captures impedance amplification
  - Accounts for frequency dependent non-linearity when coupled with PGA_{rock}
- **Caveats**
  - Does not account for detailed site specific geology
  - Defined for response spectra, applied to Fourier amplitude spectra
    - Neglects multiples/reverberations/phase modifications
    - Possible causality issues